

The Arcetri Catalog of H₂O maser sources: Update 2000^{*,**}

R. Valdetaro¹, F. Palla¹, J. Brand², R. Cesaroni¹, G. Comoretto¹, S. Di Franco³, M. Felli¹, E. Natale⁴,
F. Palagi⁴, D. Panella¹, and G. Tofani¹

¹ Osservatorio Astrofisico di Arcetri, Largo E. Fermi 5, 50125 Firenze, Italy

² Istituto di Radioastronomia CNR, Via Gobetti 101, 40129 Bologna, Italy

³ Dipartimento di Astronomia e Scienza dello Spazio, Largo E. Fermi 5, 50125 Firenze, Italy

⁴ CAISMI, C.N.R., Largo E. Fermi 5, 50125 Firenze, Italy

Received 9 August 2000 / Accepted 11 December 2000

Abstract. We present a second update of the Arcetri Catalog of water masers (Comoretto et al. 1990; Brand et al. 1994). The present study reports the results of the observations carried out with the Medicina 32-m radiotelescope from January 1993 to April 2000 on a sample of 300 sources. This compilation consists of newly discovered maser sources that did not appear in the previous Arcetri Catalogs and is made of: a) detections from the literature, and b) unpublished detections obtained with the Medicina antenna. Overall, 83 out of 300 sources were detected. The detection rate is low (28%) and we attribute this result to the inclusion in our survey of a rather large number of spurious maser detections that have appeared in one particular paper. The observational parameters are reported in tabular form for all the 300 sources and the spectra of the detected masers are presented. We discuss the global properties of the complete Arcetri Catalog based on Comoretto et al. (1990), Brand et al. (1994) and the present observations, which now contains 1013 galactic water maser sources. Of these, 937 have an IRAS counterpart within 1 arcmin from the nominal position of the maser. We establish a classification scheme based on the IRAS flux densities which allows to distinguish between water masers associated with star forming regions and late-type stars. The Arcetri Catalog represents a useful data base for systematic studies of galactic water maser sources.

Key words. astronomical data bases: catalogs – masers – ISM: molecules – radio lines: ISM – radio lines: stars

1. Introduction

The first Arcetri Catalog of H₂O maser sources was published in July 1990 (Comoretto et al. 1990). A revised version of it was given by Palagi et al. (1993), who also discussed the statistical properties of the sources. The Catalog gives the observational parameters of all 500 H₂O masers¹ with $\delta > -30^\circ$ reported in the literature up to January 1989, and re-observed with the Medicina 32-m

radio telescope (203 were detected at Medicina). After the publication of the Arcetri Catalog, a large number of new water masers were found in our own observing programs at Medicina and elsewhere. This development has prompted the compilation of a first update of the Catalog (Brand et al. 1994, hereafter U1), which contains all the sources reported in the literature from March 1989 to December 1992 as observed at Medicina. U1 gives the parameters of 213 sources² in tabular form (141 of these were detected at Medicina), bringing the size of the Arcetri Catalog to 712 masers³ (a 42% increase).

The basic motivation of the Arcetri Catalog is to provide a homogeneous and complete list of all H₂O maser “centers” observed as separate sources with the 1.9 arcmin HPBW of the 32-m Medicina telescope, and to present at

Send offprint requests to: R. Valdetaro,
e-mail: rv@arcetri.astro.it

* Based on observations collected with the Medicina 32-m radiotelescope. The Medicina telescope is operated by the Istituto di Radioastronomia, C.N.R., Bologna.

** Table 2 is only available in electronic form at the CDS via anonymous ftp to cdsarc.u-strasbg.fr (130.79.125.5) or via

<http://cdsweb.u-strasbg.fr/cgi-bin/qcat?J/A+A/368/845>

¹ Note that Comoretto et al. list 505 H₂O sources. However, five of them (HH7-11(B), M17(6), S88, IRAS 09353+0319, BFS 11(A)) are at a distance of less than 1 arcmin from another source and should not be considered as separate entries.

² U1 contains 214 sources, but one of them (IRAS 18144–1723) is already present in Comoretto et al. (1990).

³ With the criterion on distance defined in note 1, the merging of Comoretto et al. (1990) and U1 catalogs produces 712 independent entries in the Catalog instead of 713.

least one spectrum for each detected maser or an upper limit to the peak flux density for those not detected by us. Single dish and interferometric observations of higher spatial resolution have revealed the existence of many distinct components around a maser center reported in our Catalog. However, tabulation of all these finer components is beyond the scope and usefulness of our study.

There are two types of H₂O masers, those that occur in star forming regions, and those that originate in the envelopes of evolved stars. From the scientific viewpoint, the importance of studying water masers is readily understood. Masers of the first type are beacons of star formation sites, and allow one to explore the environment of deeply embedded sources, completely inaccessible at optical and near-infrared wavelengths. Knowledge of maser emission having been observed towards an IRAS source pinpoints the direction in which more detailed searches for newly formed stars should be made (e.g. Schreyer et al. 1996; Plume et al. 1997; Launhardt et al. 1998; Zinchenko et al. 1998). Stellar masers are observed to obtain knowledge of the spatial- and velocity structure of the stellar envelopes and to study their variability. When used in combination with other (optical, IR, and high-resolution radio) observations these studies yield important information on the stellar mass loss rate, the physical conditions in the circumstellar shell, and the maser pumping mechanism (e.g. Benson & Little-Marenin 1996; Lewis 1999; Colomer et al. 2000).

The availability of a catalog, in which all known water masers are brought together is an important aid to these studies, in that it greatly facilitates the selection of objects on which to perform more detailed studies. The Arcetri catalog is such a data base. Moreover, because all masers in this catalog have been re-observed with the same telescope and receiver, the data presented therein allow statistical studies (e.g. Palagi et al. 1993). The Arcetri catalog is, so to speak, only the tip of the iceberg of the complete Arcetri archive of water masers: for many sources we have continued monitoring the maser emission over the years, resulting in a coverage of more than 10 years in several cases. Thus, maser variability studies on long time scales can also be performed.

The second update of the Catalog presented here (hereafter U2) contains 300 sources which satisfy the criteria established in Comoretto et al. (1990) and in U1. These are: the distance between two maser centers should be larger than 1 arcmin and the source must have a declination $\delta > -30^\circ$. We note that such a separation represents a minimum value: when strong masers are present with intensities up to $\sim 10^5$ Jy, as in the case of Orion KL and W3OH, the appropriate distance for two sources to be considered independent becomes much larger. Work is in progress to be more quantitative. Preliminary results from a large region mapped around Orion KL indicate that the emission of the strong maser (at the same velocity) can be seen in the sidelobes of the beam pattern with an intensity above our mean noise up to distances of 30 HPBW.

The majority of the sources contained in U2 are associated with late-type stars, while the rest are IRAS sources selected for having colors typical of star forming regions (SFR). We have detected water emission in 83 sources, and their spectra, including multiple observations of the same source, are presented in Sect. 3. In total, U2 brings the total number of sources contained in the Arcetri Catalog to 1013 (423 detected at Medicina), a 42% increase with respect to U1. The global properties of the Catalog are discussed in Sect. 4.

2. Observations

All the observations reported in this paper were carried out with the Medicina 32-m radiotelescope during a number of sessions in the period January 1993–April 2000. A description of the telescope and the equipment is given by Comoretto et al. (1990), and here we will only give a summary of the main features.

At the frequency of the 6₁₆–5₂₃ transition of H₂O (22.23507985 GHz), the HPBW of the antenna is 1.9 arcmin. The pointing model was checked at the beginning of each 2–3 week session by maximizing the signal from a set of strong galactic H₂O masers (W3OH, Orion KL, Sgr B2, W49N). The resulting accuracy was always better than 25 arcsec. The antenna gain as a function of elevation was determined regularly by doing short (~ 10 min) total power integrations on DR21 (adopted flux density 18.8 Jy, Dent 1972). For each observing day, all gain measurements as a function of elevation were fitted with a polynomial curve, which was then used to calculate the conversion factor from antenna temperature to flux density for the spectra observed on that day. The calibration error resulting from the dispersion of the single measurements from the fit turns out to be 19%. On a few dates, no gain curve was measured: in these cases we have applied the closest gain curve in time and we estimate a corresponding calibration uncertainty of 7%. Therefore, a conservative estimate for such an uncertainty has to be taken equal to 21%.

Observations were always done in total power mode, with 5 min integration time on- as well as off-source. Depending on weather conditions, elevation, and spectral resolution, this resulted in 1σ rms noise levels between 0.3 Jy and 6 Jy. The distribution of the rms noise for the 426 observations (including multiple observations of the same source) is shown in Fig. 1. The peak occurs at 0.7 Jy both for positions where emission was (solid line) and was not (broken line) detected. Compared to the observations presented in U1, there is a factor of ~ 2 improvement in the rms of the present survey. In general, the band was centered on the expected velocity, either the velocity of the maser as reported in the literature, or, if available, the velocity of the molecular cloud in which the source is embedded.

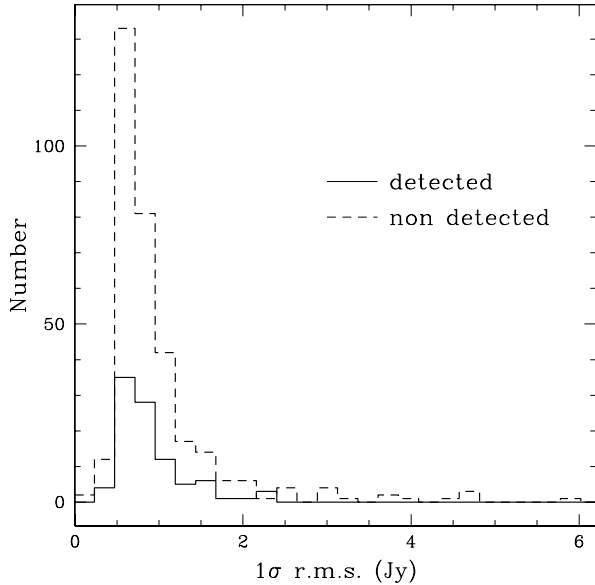


Fig. 1. The distribution of the 1σ rms noise for the 426 spectra observed in U2. The bin size is 0.25 Jy

3. Summary of results for Update2

We have collected all the information available in the literature on 300 new H₂O maser sources discovered after the completion of the first update of the Arcetri Catalog (U1). All the entries of the observed sources are listed in Table 1, which gives:

- *Columns 1 and 2:* Source names: IRAS and/or another designation;
- *Columns 3 and 4:* Equatorial Coordinates (1950 equinox);
- *Column 5:* Color-based classification of the IRAS source associated with the H₂O maser (see the Appendix);
- *Column 6:* Date of observation;
- *Column 7:* Spectral resolution in km s⁻¹;
- *Column 8:* Scan number;
- *Column 9:* 1σ rms noise level in the spectrum;
- *Columns 10 to 14:* Parameters of the H₂O maser emission. We give the minimum and maximum velocity of the emission, the velocity of the peak signal, the peak flux density, and the integrated flux, respectively. In the case of no detection, the minimum and maximum velocities indicate the total velocity extent of the spectrum. The parameters were estimated by visual inspection of the spectra. Obviously, this is a subjective method, and we suggest the reader to consult the spectra of the detections, all of which are shown in Fig. A.2. The uncertainty in the peak flux density is taken to be equal to the maximum between the rms given in Col. 9 and the calibration error discussed in Sect. 2. The error in the integrated flux density is dominated by the uncertainty in the calibration. The error in velocity can be assumed equal to the corresponding spectral resolution, given in Col. 7;

- *Column 15:* Each entry is the coded reference to the publication in which the maser was first reported. No attempt was made to list all publications pertaining to a particular source. The reference codes are a continuation of those used in Comoretto et al. (1990) and U1, and are specified at the bottom of Table 1.

As in U1, we have classified each maser source following the scheme introduced by Palagi et al. (1993). A full explanation of the criteria adopted to distinguish objects based on the IRAS colors is given in the Appendix. Based on the fluxes in the four IRAS bands, two classes are readily identified: late-type stars (STAR) and star forming regions (SFR). In case of no assignment, the source is labeled as *unknown* (UNKN) or *strange* (STRN) (see Appendix).

Almost all sources in Table 1 have an IRAS point source as a counterpart (289 out of 300 entries). This is not surprising, since the input source lists for water maser studies are typically derived from the IRAS PSC. For the 11 sources without counterpart within 1 arcmin, we have searched in the IRAS catalog doubling the radius around the maser position, with no success. Overall, the classification criteria yield the following results: 201 STAR, 75 SFR, 10 UNKN, 3 STRN. The large number of STAR masers reflects the fact that recent studies have concentrated on H₂O masers associated with late-type stars.

Of the 300 sources, 83 (28%) were detected at least once at Medicina during the period 01/1993–04/2000. About two thirds of the 300 sources were observed only once (199); of these, 59 (30%) were detected. More than half (33) of these 59 are associated with long-period variables, the rest are SFR (20) and UNKN (6). Spectra of all the detections are shown in Fig. A.2. The identification is by scan number (upper left) and source name (upper right). Note that, in order to make the spectra readable, only part of the velocity range covered in our observations is shown in the figure.

Table 1 contains 7 new water maser sources discovered during the course of a dedicated project aimed at studying the frequency of maser occurrence among 91 bright IRAS sources ($F_{60\ \mu\text{m}} \geq 100$ Jy) with colors corresponding to those of ultracompact HII regions (Wood & Churchwell 1989). These 91 sources had been already observed in 1989–90 and were reported in Palla et al. (1991) as non-detections. The newly detected sources are: IRAS 18372–0541, IRAS 19368+2239, IRAS 19560+3135, IRAS 20307+3749, IRAS 22267+6244, IRAS 22480+6002, IRAS 23545+6508. Another new detection is also listed in Table 1 as G23.27+0.08 (Codella & Moscadelli 2000).

Figure 2 shows the distribution of the peak flux densities (taken from the literature) of the sources that were *not* detected in the present survey. We see that the distribution is unusually bimodal. The peak below ~ 1 Jy is expected, as it corresponds to the average 1σ rms of our observations (see Table 1). The second peak at ~ 30 Jy, instead, is totally unexpected: however, this is determined by the non-detections obtained towards the sample of Han et al. (1995), as clearly demonstrated by the fact that such

Table 1. Arcetri update 2000

IRAS (1)	Other (2)	RA (1950) (3)	DEC (1950) (4)	Class (5)	Date (6)	ΔV (km s ⁻¹) (7)	Scan (8)	rms (Jy) (9)	V_{\min} (km s ⁻¹) (10)	V_{\max} (km s ⁻¹) (11)	V_{peak} (km s ⁻¹) (12)	F_{ν}^{peak} (Jy) (13)	$\int F_{\nu} dV$ (Jy km s ⁻¹) (14)	Ref. ^(a) (15)
00067+6340		00:06:47.7	+63:40:34	STAR	13/03/97	0.263	56005	0.75	-140	80				104
					20/01/99	0.263	74103	0.55	-180	80				
00087+5833	LkH α 198	00:08:47.9	+58:33:09	SFR	13/03/97	0.263	56059	1.85	-140	80				104
					07/05/97	0.263	59295	1.07	-140	80				
					20/01/99	0.263	74105	0.49	-120	150				
00213+6530		00:21:22.0	+65:30:25	UNKN	13/03/97	0.263	56061	1.25	-110	110				104
					07/05/97	0.263	59297	1.11	-110	110				
					19/01/99	0.263	73954	0.62	-130	130				
00213+3818		00:21:23.1	+38:18:00	STAR	07/05/97	0.263	59299	1.46	-120	120				104
					19/01/99	0.263	73956	0.68	-160	100				
01265+4624	CE And	01:26:33.5	+46:24:06	STAR	27/12/99	0.263	79036	0.78	-15	-11	-13.2	10	10	118
01597+1601	RY Ari	01:59:45.9	+16:01:52	STAR	27/12/99	0.263	79038	0.64	-120	110				118
					19/01/99	0.263	73960	0.62	-115	130				
02145+7831	AG Cep	02:14:33.8	+78:31:48	STAR	27/12/99	0.263	79040	0.68	-120	120				110
02252+6120	IC 1805	02:25:14.5	+61:20:10	UNKN	19/01/99	0.263	73964	0.60	-110	110				100
02270-2619	R For	02:27:01.2	-26:19:18	STAR	05/05/97	0.263	59122	2.47	-101	115				104
02293+5748		02:29:21.0	+57:48:51	STAR	13/03/97	0.263	56007	0.94	-117	99				104
					19/01/99	0.263	73966	0.62	-150	40				
02302+4525	UX And	02:30:12.0	+45:25:59	STAR	27/12/99	0.263	79042	0.81	-120	120				110
02455+6034		02:45:30.0	+60:34:35	SFR	13/03/97	0.263	56009	0.90	-130	86				104
					19/01/99	0.263	73968	0.57	-130	86				
02455+1718	T Ari	02:45:32.0	+17:18:06	STAR	27/12/99	0.263	79044	0.70	-130	115				113
02469+5646	W Per	02:46:55.0	+56:46:35	STAR	27/12/99	0.263	79046	0.81	-170	90				115
03064+5638		03:06:26.8	+56:38:56	SFR	13/03/97	0.263	56011	0.85	-71	143				104
					19/01/99	0.263	73970	0.67	-71	143				
03094+5530		03:09:27.1	+55:30:56	STAR	13/03/97	0.263	56013	0.91	-94	121				104
					19/01/99	0.263	75979	0.68	-147	120				
	L1448	03:22:34.3	+30:33:35		02/07/97	0.263	60797	1.50	-100	100				107
					17/03/98	0.263	69097	1.35	-103	109				
					19/01/99	0.263	73983	0.65	-155	112				

IRAS (1)	Other (2)	RA (1950) (3)	DEC (1950) (4)	Class (5)	Date (6)	ΔV (km s ⁻¹) (7)	Scan (8)	rms (Jy) (9)	V_{\min} (km s ⁻¹) (10)	V_{\max} (km s ⁻¹) (11)	V_{peak} (km s ⁻¹) (12)	F_{ν}^{peak} (Jy) (13)	$\int F_{\nu} dV$ (Jy km s ⁻¹) (14)	Ref. ^(a) (15)
03258+3104	N1333IRS2	03:25:49.9	+31:04:16	SFR	18/01/94	0.165	32880	0.4	-18.2	-12.3	-16.4	3	7	105
					02/07/97	0.263	60799	1.54	-100	100				
	OH141.7	03:29:08.9	+60:10:18		13/03/97	0.263	56015	0.92	-136	79				104
					05/05/97	0.263	59144	1.40	-136	79				
					01/19/99	0.263	73987	0.62	-188	79				
03385+5927		03:38:34.1	+59:27:30	STAR	13/03/97	0.263	56017	0.89	-118	98				104
					05/05/97	0.263	59146	1.30	-118	98				
					19/01/99	0.263	73989	0.63	-165	93				
03414+3200		03:41:28.0	+32:00:01	SFR	13/03/97	0.263	56019	0.88	-87	129				104
					05/05/97	0.263	59148	1.26	-87	129				
					19/01/99	0.263	73991	0.58	-136	124				
03453+3207		03:45:23.3	+32:07:33	STAR	27/12/99	0.263	79048	0.81	-43	-19	-22	2	2	117
03507+3623	IRC+40072	03:50:46.2	+36:23:28	STAR	27/12/99	0.263	79050	0.73	-100	-84	-92	7	21	110
03598-1353	WZ Eri	03:59:49.0	-13:53:16	STAR	27/12/99	0.263	79052	1.6	-120	95				111
04016+2610	L1489	04:01:40.6	+26:10:48	SFR	13/03/97	0.263	56021	0.67	-150	64				104
					05/05/97	0.263	59150	1.34	-149	64				
					04/08/98	0.132	71029	1.71	-39	67				
					19/01/99	0.263	73993	0.63	-198	60				
04034+5116		04:03:23.8	+51:16:45	SFR	13/03/97	0.263	56023	0.90	-186	29				104
					05/05/97	0.263	59152	1.35	-186	29				
					19/01/99	0.263	73995	0.55	-186	29				
04157-1837	RS Eri	04:15:42.5	-18:37:42	STAR	18/01/00	0.263	79408	1.10	46.9	51.5	49.6	41	58	110
04166+4056	IR Per	04:16:36.5	+40:56:37	STAR	27/12/99	0.263	79054	0.78	-140	60				115
04260+2437	IRC+20082	04:26:05.6	+24:37:16	STAR	27/12/99	0.263	79056	0.69	-110	90				110
	G165.35-9.03	04:26:50.0	+35:09:24		13/03/97	0.263	56025	1.04	-150	65				104
					19/01/99	0.263	73997	0.60	-199	60				

a peak disappears once these sources are removed from the distribution (dashed histogram in Fig. 2). We thus conclude that the large majority of the detections obtained by Han et al. (1995) are likely to be spurious. Such a conclusion is reinforced by the fact that out of the 13 sources of Han et al. detected at Medicina, only 7 show emission

within 50 km s⁻¹ from the velocity quoted by Han et al., and for 4 of these the velocity difference is ≥ 19 km s⁻¹.

4. Global properties of the Arcetri Catalog

A computer-readable version of Table 1, plus the amended version of Table 2 of Comoretto et al. (1990) and Table 1

Table 1. continued

Source (1)	Other (2)	RA (1950) (3)	DEC (1950) (4)	Class (5)	Date (6)	ΔV (km s ⁻¹) (7)	Scan (8)	rms (Jy) (9)	V_{\min} (km s ⁻¹) (10)	V_{\max} (km s ⁻¹) (11)	V_{peak} (km s ⁻¹) (12)	F_{ν}^{peak} (Jy) (13)	$\int F_{\nu} dV$ (Jy km s ⁻¹) (14)	Ref. ^(a) (15)
04287+1807	XZ Tau	04:28:44.4	+18:07:36	SFR	13/03/97 04/08/98 19/01/99	0.263 0.132 0.263	56027 71033 73999	0.85 1.68 0.60	-135 -41 -100	81 68 120				104
04311-0004	BD Eri	04:31:11.0	-00:04:36	STAR	27/12/99	0.263	79058	0.89	-120	100				111
04325+2402	L1535	04:32:31.6	+24:02:08	SFR	13/03/97 21/01/99	0.263 0.263	56029 74217	0.71 0.55	-107 -155	110 104				104
04382-1417	BX Eri	04:38:14.8	-14:17:47	STAR	27/12/99	0.263	79060	1.6	-110	110				118
04393-0802		04:39:23.2	-08:02:59	STAR	05/04/00	0.263	80416	1.6	-75	135				118
	R Lep	04:57:19.7	+14:52:46		20/01/99	0.263	74115	1.25	60	160				104
05104+2055		05:10:26.0	+20:55:59	STAR	13/03/97 21/01/99	0.263 0.263	56031 74219	0.73 0.62	-120 -167	96 90				104
05220-0611	EX Ori	05:22:00.8	-06:11:31	STAR	27/12/99	0.263	79064	1.1	-160	80				110
05281+3412		05:28:07.7	+34:12:46	SFR	13/03/97 21/01/99	0.263 0.263	56033 74225	0.98 0.54	-63 -112	152 147				104
05338-0624	L1641 N	05:33:54.7	-06:23:58	SFR	20/01/99	0.263	74119	0.50	-118	142				100
05354+2458		05:35:28.2	+24:58:26	STAR	13/03/97 21/01/99	0.263 0.263	56035 74229	0.73 0.52	-1.2 -4.3	6.0 6.4	2.9 1.2	23 5	24 10	104
05358-0704	Haro4-13A	05:35:55.3	-07:04:41	SFR	13/03/97 21/01/99	0.263 0.263	56037 74231	0.91 0.76	-126 -130	89 130				104
05369-0728	Haro4-13 NGC2023	05:36:56.4 05:39:04.1	-07:28:14 -07:17:56	SFR	05/04/00 20/01/99	0.263 0.263	80432 74121	1.40 0.59	-85 -117	110 142				107 100
05423+2905		05:42:18.9	+29:05:54	STAR	27/12/99	0.263	79066	0.80	19	27	23.7	3	9	112
05480+2545		05:48:01.9	+25:44:50	STRN	19/01/94 22/03/99	0.165 0.263	32988 74960	0.87 0.78	-93 -134	76 133				110
05554+2013		05:55:26.2	+20:13:45	SFR	13/03/97 21/01/99	0.263 0.263	56039 74239	0.74 0.68	-175 -224	39 34				104
06048+1839	LkH α 208	06:04:53.2	+18:39:55	SFR	13/03/97 21/01/99	0.263 0.263	56041 74241	0.76 0.85	-188 -139	29 129				104
06068+2030		06:06:53.0	+20:30:41	SFR	13/03/97 21/01/99	0.263 0.263	56043 74243	0.72 0.62	-151 -199	63 58				104

Source (1)	Other (2)	RA (1950) (3)	DEC (1950) (4)	Class (5)	Date (6)	ΔV (km s ⁻¹) (7)	Scan (8)	rms (Jy) (9)	V_{\min} (km s ⁻¹) (10)	V_{\max} (km s ⁻¹) (11)	V_{peak} (km s ⁻¹) (12)	F_{ν}^{peak} (Jy) (13)	$\int F_{\nu} dV$ (Jy km s ⁻¹) (14)	Ref. ^(a) (15)
06183+1135		06:18:19.3	+11:35:42	STAR	13/03/97 05/05/97 21/01/99	0.263 0.263 0.263	56045 59154 74245	0.87 1.25 1.00	-94 -93 -143	122 122 116				104
06190+1040		06:19:01.3	+10:40:51	SFR	23/04/93 21/01/99	0.329 0.263	28736 74247	2.89 0.50	-168 -129	168 128				101
06278+2729	DW Gem	06:27:51.3	+27:29:16	STAR	27/12/99	0.263	79068	0.77	-120	120				118
06304+6407	RT Cam	06:30:29.0	+64:07:57	STAR	18/01/00	0.263	79400	0.61	-110	60				111
06349-0121	SY Mon	06:34:59.0	-01:21:05	STAR	18/01/00	0.263	79434	0.64	-100	0				111,114
06423+0905	FX Mon	06:42:21.5	09:05:27	STAR	18/01/00	0.263	79436	0.53	32.2	36.5	35.2	4	5	110
06567-0350	BFS 56	06:56:45.1	-03:50:41	SFR	13/03/97 05/04/00	0.263 0.263	56051 80420	0.88 1.06	-96 -90	121 105				104
06568-1154	CMA-W	06:56:52.9	-11:54:46	SFR	13/03/97 21/01/99	0.263 0.263	56053 74253	1.09 1.01	-115 -129	101 129				104
06571-0441	S287-B	06:57:06.4	-04:41:48	SFR	13/03/97 21/01/99	0.263 0.263	56055 74255	0.94 0.61	-132 -180	84 79				104
06572-0742	L1654	06:57:16.8	-07:42:16	SFR	13/03/97 19/01/99	0.263 0.263	56057 74003	1.30 0.58	-106 -130	109 129				104
07331+0021	AI CMi	07:33:07.0	+00:21:40	STRN	18/01/00	0.263	79438	0.70	-80	140				112
07333-1838		07:33:21.3	-18:38:51	SFR	19/01/99	0.263	74007	1.37	-138	119				104
07445-2613	CRL1192	07:44:34.0	-26:13:11	STAR	13/03/97 19/01/99	0.263 0.263	56049 74013	1.88 3.12	76.6 -52	84.9 208	81.5	19	50	104
08149-1338	SV Pup	08:14:57.9	-13:38:57	STAR	18/01/00	0.263	79440	0.82	-10	100				110
08272-0609	RT Hya	08:27:13.2	-06:09:01	STAR	18/01/00	0.263	79442	0.74	0	100				115
09057+1325	CW Cnc	09:05:42.1	+13:25:23	STAR	18/01/00	0.263	79444	0.59	-95	100				118
09076+3110	RS Cnc	09:07:37.7	+31:10:04	STAR	18/01/00	0.263	79446	0.60	-110	100				115
09452+1330	IRC+10216	09:45:14.1	+13:30:40	STAR	11/03/97 19/01/99	0.263 0.263	55761 74015	0.86 0.69	-83 -130	128 127				104
09507+3509	S LMi	09:50:45.0	+35:09:42	STAR	18/01/00	0.263	79310	0.64	-100	100				111

of U1 is published electronically. The combined Table 2 contains all the 1013 sources observed at Medicina (423 detected) and lists one entry per source, usually the one with the highest flux density observed at Medicina.

Many sources have multiple observations in our database, in some cases covering a period of more than

10 years. An analysis of the variability of the maser emission for a subset of sources with the longest time coverage and largest sampling is under way (Valdetaro et al., in preparation). Information on multiple observations of selected sources can be obtained upon request to palagi@arcetri.astro.it.

Table 1. continued

Source (1)	Other (2)	RA (1950) (3)	DEC (1950) (4)	Class (5)	Date (6)	ΔV (km s ⁻¹) (7)	Scan (8)	rms (Jy) (9)	V_{\min} (km s ⁻¹) (10)	V_{\max} (km s ⁻¹) (11)	V_{peak} (km s ⁻¹) (12)	F_{ν}^{peak} (Jy) (13)	$\int F_{\nu} dV$ (Jy km s ⁻¹) (14)	Ref. ^(a) (15)
10132+3049	CIT 6	10:13:11.0	+30:49:17	STAR	20/01/99	0.263	74017	0.55	-107	152				104
11308-1020		11:30:52.3	-10:20:26	STAR	25/01/99	0.263	74459	4.67	-108	151				104
11445+4344		11:44:36.0	+43:44:57	STAR	11/03/97	0.263	55763	1.00	-176	35				104
					22/01/99	0.263	74281	0.47	-103.4	-96.1	-100.2	20	11	
12380+5607	Y UMa	12:38:03.5	+56:07:19	STAR	11/03/97	0.263	55765	0.90	-82	128				104,115
					22/01/99	0.263	74285	0.62	-131	128				
13114-0232	SW Vir	13:11:29.7	-02:32:34	STAR	11/03/97	0.263	55767	0.82	-98	114				104,110
					22/01/99	0.263	74287	0.54	-144	114				
14086-0730	OH 334	14:08:40.0	-07:30:42	STAR	27/12/99	0.263	79072	0.95	-23	-15	-19	4	6	111
14280-2952	Y Cen	14:28:01.1	-29:52:32	STAR	06/04/00	0.263	80467	4.65	-100	105				110
14524-2148	EG Lib	14:52:28.9	-21:48:14	STAR	27/12/99	0.263	79076	3.29	-120	120				110
15410-0133	BG Ser	15:41:00.3	-01:33:09	STAR	27/12/99	0.263	79080	0.75	-4.0	0.2	-1.9	7	10	110
16011+4722	X Her	16:01:07.9	+47:22:36	STAR	14/03/97	0.263	56087	1.07	-150	66				104,115
					03/05/97	0.263	56738	1.30	-203	66				
					21/01/99	0.263	74143	0.47	-180	50				
16146-2246	S Sco	16:14:42.0	-22:46:18	STAR	27/12/99	0.263	79084	5.9	60	290				111
16231-2427	S-R3	16:23:07.7	-24:27:26	UNKN	22/05/93	0.263	56089	1.48	-107	109				104
	GSS30	16:23:20.0	-24:16:18		06/04/00	0.263	80471	3.91	-85	105				120
	VLA1623	16:23:25.0	-24:17:47		06/04/00	0.263	80473	2.98	-95	105				120
16313-1703	S Oph	16:31:21.9	-17:03:30	STAR	27/12/99	0.263	79086	1.7	-80	120				111
	RNO90	16:31:38.0	-15:42:04		14/03/97	0.263	56091	1.12	-56	160				104
16442-0930	L255	16:44:14.2	-09:30:03	SFR	14/03/97	0.263	56093	1.15	-140	75				104
					03/05/97	0.263	58736	1.02	-198	76				
					21/01/99	0.263	74033	0.55	-19.5	-9.4	-13.4	2	5	
17034-1024	V850 Oph	17:03:24.9	-10:24:59	STAR	27/12/99	0.263	79090	0.99	-110	90				111
17049-2440	AFGL 1922	17:04:54.3	-24:40:29	STAR	06/04/00	0.263	80475	3.61	-90	105				104
17103-0559		17:10:18.5	-05:59:29	STAR	14/03/97	0.263	56095	0.92	-109	107				104
					21/01/99	0.263	74151	0.53	-156	102				

Source (1)	Other (2)	RA (1950) (3)	DEC (1950) (4)	Class (5)	Date (6)	ΔV (km s ⁻¹) (7)	Scan (8)	rms (Jy) (9)	V_{\min} (km s ⁻¹) (10)	V_{\max} (km s ⁻¹) (11)	V_{peak} (km s ⁻¹) (12)	F_{ν}^{peak} (Jy) (13)	$\int F_{\nu} dV$ (Jy km s ⁻¹) (14)	Ref. ^(a) (15)
17162-1934	V1848 Oph	17:16:15.0	-19:34:42	STAR	27/12/99	0.263	79094	2.04	-150	90				111
17190+2658	V393 Her	17:19:04.0	+26:58:42	STAR	27/12/99	0.263	79096	0.55	-90	150				111
17334+1537		17:33:24.9	+15:37:02	STAR	14/03/97	0.263	56097	0.82	-81	135				104
					21/01/99	0.263	74153	0.46	-100	120				
17343+1052	V790 Oph	17:34:24.0	+10:52:52	STAR	27/12/99	0.263	79098	0.51	-60	-53	-57.0	20	23	111
17445-2900		17:44:33.5	-29:00:03	UNKN	06/04/00	0.263	80477	4.45	-95	105				103
17554+2946	AU Her	17:55:24.0	+29:46:45	STAR	27/12/99	0.263	79100	0.71	-140	90				111,112
17581-1744		17:58:11.3	-17:44:20	STAR	20/01/99	0.263	74037	2.49	-124	145				104
18018-2802	V1804 Sgr	18:01:51.9	-28:02:10	STAR	06/04/00	0.263	80479	4.80	-95	105				113
18033+2229		18:03:18.3	+22:29:38	STAR	15/01/00	0.263	79213	0.61	22.4	27.9	24.2	2	7	112
18052-2205		18:05:16.9	-22:05:42	SFR	21/01/99	0.263	74155	0.87	-95.4	-89.6	-94.7	15	12	103
18061-1927		18:06:09.6	-19:27:56	UNKN	06/04/00	0.263	80481	2.20	11.3	26.0	21.7	59	124	103
18083-2630	CRL2086	18:08:20.0	-26:30:18	STAR	14/03/97	0.263	56099	1.95	-128	88				104
18085+0752	XY Oph	18:08:34.5	+07:52:25	STAR	15/01/00	0.263	79215	0.90	-70.6	-62.5	-67.9	10	10	112
18099+3127		18:09:55.0	+31:27:30	STAR	06/06/00	0.263	80485	1.17	16.3	29.6	19.2	5	22	112
18112-1801		18:11:12.3	-18:01:16	UNKN	06/04/00	0.263	80487	2.00	-70	105				103
18148-0440	L 483	18:14:50.4	-04:40:15	SFR	20/01/99	0.263	74039	1.34	-2.1	2.1	0.3	23	18	100
18151-1208		18:15:09.0	-12:08:33	SFR	25/01/94	0.165	33535	1.47	28	33.7	30.3	33	48	105
18151-1134		18:15:09.4	-11:34:44	SFR	25/01/94	0.165	33546	1.48	-56	112				105
					21/01/99	0.263	74163	0.70	-90	150				
18156-0653		18:15:36.9	-06:53:06	STAR	14/03/97	0.263	56101	0.92	-142	74				104
					22/01/99	0.263	74291	1.61	-95.9	-88.3	-91.0	20	17	
18186+3143	TU Lyr	18:18:37.6	+31:43:54	STAR	15/01/00	0.263	79219	0.74	0	11	5.9	9	33	118
18196-1331	OH17.6	18:19:37.0	-13:31:47	SFR	18/01/00	0.263	79322	2.38	23	31	27.1	330	360	111
18213+0335	V2090 OPH	18:21:22.9	+03:35:42	STAR	18/01/00	0.263	79324	0.71	-120	80				118
18236+0706		18:23:41.5	+07:06:47	STAR	18/01/00	0.263	79326	0.76	-30	250				112
18250-0351		18:25:00.4	-03:51:49	SFR	14/03/97	0.263	56103	0.85	-185	32				104
					22/01/99	0.263	74295	1.56	-232	27				
18251+0023		18:25:10.5	+00:23:18	STAR	18/01/00	0.263	79328	0.67	-10	160				112
18252+1305		18:25:15.2	-13:05:37	STAR	14/03/97	0.263	56105	1.03	22.7	65	27.0	19	42	104
					06/04/00	0.263	80489	2.00	-50	130				

Of the 1013 masers listed in the Arcetri catalog, 937 have an associated IRAS source. According to the classification criteria introduced in the previous section and in Appendix A, we find that the 937 masers are partitioned in the following way: 410 SFR, 460 STAR, 61 UNKN, 6 STRN. In Fig. 3 we show the IRAS color-color plot using the variables u_4 and u_5 defined in the Appendix. Note

that the advantage of this classification over the more conventional two-color IRAS diagrams is that it exploits the information provided by the four far-infrared bands simultaneously. Also, sources with upper limits can be more properly treated (see Appendix). Water masers associated with SFR and STAR are well separated in this diagram. Figure 3 also indicates that the distribution of the UNKN

Table 1. continued

Source (1)	Other (2)	RA (1950) (3)	DEC (1950) (4)	Class (5)	Date (6)	ΔV (km s ⁻¹) (7)	Scan (8)	rms (Jy) (9)	V_{\min} (km s ⁻¹) (10)	V_{\max} (km s ⁻¹) (11)	V_{peak} (km s ⁻¹) (12)	F_{ν}^{peak} (Jy) (13)	$\int F_{\nu} dV$ (Jy km s ⁻¹) (14)	Ref. ^(a) (15)
18262+0006	VV Ser	18:26:14.3	+00:06:39	SFR	14/03/97	0.263	56107	0.89	-37	179				104
18265-1517	L379-IRS3	18:26:32.5	-15:17:17	SFR	22/01/99	0.263	74299	0.92	-84	174				100
18273-0738		18:27:24.0	-07:38:57	STAR	20/01/99	0.263	74041	1.53	-184	83	-19.4	11	34	104
18276+0839	V 603 Oph	18:27:39.7	+08:39:18	STAR	14/03/97	0.263	56109	1.00	-139	76				104
18303-0519		18:30:20.4	-05:19:42	STAR	22/01/99	0.263	74301	1.13	-186	72				104
18306-0835	G23.27+0.08	18:30:40.0	-08:35:53	SFR	18/01/00	0.263	79332	1.08	68	71	69.8	170	170	112
18308-0503		18:30:50.8	-05:03:26	SFR	14/03/97	0.263	56111	1.04	-93	123				104
18317-0845		18:31:45.8	-08:45:47	SFR	22/01/99	0.263	74307	0.72	-141	118				104
18317-0513		18:31:46.1	-05:13:23	SFR	22/04/93	0.329	28393	0.49	75.7	82.7	77.0	8.1	17.9	119
18321-0854		18:32:07.7	-08:54:05	UNKN	18/01/93	0.329	26667	1.41	28.2	67.7	53.7	45	120	103
18324-0820		18:32:27.2	-08:20:23	SFR	22/01/99	0.263	74305	0.82	-128	129				104
18341+0005		18:34:07.3	+00:05:28	STAR	14/03/97	0.263	56113	0.92	-112	103				104
18355+0227		18:35:34.5	+02:27:17	STAR	22/01/99	0.263	74309	0.78	-161	98				104
18356-0951		18:35:40.3	-09:51:42	STAR	20/01/94	0.165	33053	0.98	42.5	46.8	44.6	44	38	105
18361-0627		18:36:10.5	-06:27:44	SFR	19/03/99	0.263	74870	0.64	41.5	63.8	44.9	68	85	105
18362+0538		18:36:14.7	+05:38:41	STAR	19/01/93	0.329	26878	1.19	76.8	81.1	79	11	13.2	103
18372-0541		18:37:15.5	-05:41:33	SFR	06/04/00	0.263	80491	1.57	54.8	80.6	78.9	9	27	103
18397+1738	IRC+20370	18:39:41.6	+17:38:16	STAR	14/03/97	0.263	56115	0.86	-149	67				104
18397+0758		18:39:43.9	+07:58:13	STAR	22/01/99	0.263	74315	0.64	-196	62				104
18403-0417		18:40:19.4	-04:17:01	SFR	18/01/00	0.263	79334	0.69	-50	150				104
					18/01/00	0.263	79336	0.63	0	150				104
					14/03/97	0.263	56117	0.91	-139	75				104
					22/01/99	0.263	74319	0.61	-188	70				104
					06/12/93	0.165	31756	1.62	82.1	93.4	91.1	10	26	101
					22/01/99	0.263	74321	0.59	88.3	95.4	92.0	4	6	101
					18/01/00	0.263	79338	0.68	-60	110				112
					18/01/94	0.329	32827	1.03	-168	169				120
					19/03/99	0.263	74874	0.72	20.3	27.7	23.4	10	19	104
					19/01/99	0.263	73926	0.63	-140	100				104
					18/01/00	0.263	79340	0.60	-200	0				112
					24/04/93	0.329	28787	1.02	-168	169				104
					14/03/97	0.263	56119	0.85	-132	83				104
					22/01/99	0.263	74323	0.59	-129	131				104

Source (1)	Other (2)	RA (1950) (3)	DEC (1950) (4)	Class (5)	Date (6)	ΔV (km s ⁻¹) (7)	Scan (8)	rms (Jy) (9)	V_{\min} (km s ⁻¹) (10)	V_{\max} (km s ⁻¹) (11)	V_{peak} (km s ⁻¹) (12)	F_{ν}^{peak} (Jy) (13)	$\int F_{\nu} dV$ (Jy km s ⁻¹) (14)	Ref. ^(a) (15)
18403-0445		18:40:20.7	-04:45:01	SFR	22/01/99	0.263	74325	0.63	-129	130				103
18408+0730		18:40:53.8	+07:30:11	STAR	05/04/00	0.263	80378	2.50	-100	90				112
18414-0339		18:41:28.9	-03:39:52	SFR	18/01/00	0.263	79342	0.60	-50	120				103
					28/01/93	0.329	27739	0.77	99	140	138	13	35	103
					07/05/93	0.330	28999	0.94	111.1	145.6	135	8	45	103
					22/01/99	0.263	74329	0.62	104	127	125	13	30	103
18415+0404		18:41:35.7	+04:04:14	STAR	18/01/00	0.263	79344	0.58	-70	100				112
18421-0404		18:42:10.1	-04:04:38	SFR	28/01/93	0.329	27741	3.0	-168	169				104
					14/03/97	0.263	56121	0.87	-45	171				104
					22/01/99	0.263	74331	0.61	-94	166				104
18431-0312		18:43:09.5	-03:12:37	SFR	28/01/93	0.329	27743	1.17	-168	169				104
					14/03/97	0.263	56123	0.22	-137	80				104
					05/04/00	0.263	80380	2.39	-100	105				104
18432+1343		18:43:17.3	+13:43:08	STAR	18/01/00	0.263	79346	0.54	45.0	49.1	47.0	3	5	117
18444+0734		18:44:24.1	+07:34:53	STAR	18/01/00	0.263	79348	0.61	33.4	40.4	35.8	5	10	112
18449-0158		18:44:59.5	-01:58:47	SFR	16/01/93	0.329	26622	1.21	99.8	106.5	101.7	6	29	104,103
					14/03/97	0.263	56125	0.88	-111	103				104
					21/01/99	0.263	74171	0.57	-140	80				104
18454-0136		18:45:28.0	-01:36:46	SFR	14/03/97	0.263	56127	0.81	-127	89				104
					21/01/99	0.263	74175	0.56	-174	103				104
18487+0617		18:48:47.4	+06:17:56	STAR	18/01/00	0.263	79350	0.64	70	190				112
18513+0235		18:51:22.9	+02:35:13	STAR	19/01/00	0.263	79454	0.77	30	130				116,117
18525+0210		18:52:33.5	+02:10:48	STAR	19/01/00	0.263	79456	0.69	30	130				112
18530+0215		18:53:03.0	+02:15:13	SFR	15/10/93	0.329	30397	1.90	-167	169				104
					14/03/97	0.263	56129	0.81	-151	64				104
					21/01/99	0.263	74179	0.63	-198	60				104
18542+0940		18:54:13.4	+09:40:01	STAR	19/01/00	0.263	79458	0.60	-100	0				112
18551+1345		18:55:08.8	+13:45:05	STAR	14/03/97	0.263	56131	0.85	-90	126				104
					21/01/99	0.263	74181	0.55	-137	121				104
18553+0414		18:55:23.8	+04:14:00	SFR	21/01/99	0.263	74183	0.61	0.8	19.6	10.5	50	140	103
18554+0231		18:55:25.6	+02:31:10	STAR	19/01/00	0.263	79460	0.58	-100	0				112
18561+1642	EU Aql	18:56:09.0	+16:42:43	STAR	19/01/00	0.263	79462	0.52	-40	100				111

sources overlaps that of the SFR-type, indicating a similar nature. On the other hand, the six STRN sources are equally distributed between STAR and SFR.

The distribution of the 937 sources with IRAS counterpart in the [60-12] vs. [25-12] diagram is displayed in Fig. 4. IRAS sources associated with SFR are

Table 1. continued

Source (1)	Other (2)	RA (1950) (3)	DEC (1950) (4)	Class (5)	Date (6)	ΔV (km s ⁻¹) (7)	Scan (8)	rms (Jy) (9)	V_{\min} (km s ⁻¹) (10)	V_{\max} (km s ⁻¹) (11)	V_{peak} (km s ⁻¹) (12)	F_p^{peak} (Jy) (13)	$\int F_\nu dV$ (Jy km s ⁻¹) (14)	Ref. ^(a) (15)
18563+0428		18:56:23.8	+04:28:03	SFR	16/01/93	0.329	26626	1.50	15.5	22.0	18.8	140	160	103
					21/01/99	0.263	74185	0.68	14.5	30.2	18.5	240	240	
18566+0408		18:56:40.7	+04:08:03	SFR	21/01/99	0.263	74187	0.71	-129	129				102
18568+0550		18:56:52.9	+05:50:28	STAR	19/01/00	0.263	79464	0.57	-160	0				112
18572+0618		18:57:13.7	+06:18:48	UNKN	19/01/00	0.263	79466	0.61	-100	100				112
18578+0831		18:57:53.4	+08:31:15	STAR	19/01/00	0.263	79468	0.59	0	100				112
19007+1652		19:00:46.8	+16:52:02	STAR	19/01/00	0.263	79470	0.48	-50	50				112
19008+0726	IRC+10401	19:00:52.8	+07:26:15	STAR	19/01/99	0.263	73928	0.61	-140	90				104
19010+1307		19:01:02.4	+13:07:29	STAR	19/01/00	0.263	79474	0.55	-60	140				112
19012+0505		19:01:15.5	+05:05:18	SFR	14/03/97	0.263	56133	0.90	33.1	35.5	34.0	4	3	104
					21/01/99	0.263	74189	0.67	35.0	46.7	37.3	4	6	
19035+0451		19:03:30.4	+04:51:04	STAR	19/01/00	0.263	79476	0.65	80	94	83.7	8	24	112
19041+1734		19:04:10.8	+17:34:47	STAR	19/01/00	0.263	79478	0.50	-50	90				112
19052+0922		19:05:15.8	+09:22:28	STAR	19/01/00	0.263	79484	0.53	5.6	12.4	10.1	5	11	112
19054+0419		19:05:26.2	+04:19:00	STAR	26/01/00	0.263	80040	1.14	-150	70				112
19057+0141		19:05:46.4	+01:41:37	STAR	25/01/00	0.263	79918	0.63	-55	140				112
19068+1127		19:06:50.2	+11:27:52	STAR	25/01/00	0.263	79920	0.56	-11.2	-0.8	-8.3	7	23	112
	OH 42.75	19:06:51.0	+08:04:50	STAR	25/01/00	0.263	79922	0.59	5.0	13.1	9.9	45	120	111
19071+2934	V Lyr	19:07:07.0	+29:34:42	STAR	14/03/97	0.263	56135	0.86	-14.2	-11.4	-12.6	2	4	104
					22/01/99	0.263	74333	0.53	-17.2	-10.2	-14.2	3	12	
19081+0322		19:08:06.5	+03:22:04	STAR	25/01/00	0.263	79924	0.63	0	100				112
19081+0903		19:08:09.7	+09:03:28	SFR	24/04/93	0.329	28752	1.16	-124	60	10.3	140	920	102
					22/01/99	0.263	74335	0.75	-130	130	9.4	320	1770	
19085+0755		19:08:30.6	+07:55:12	SFR	25/01/00	0.263	79926	0.53	7.2	11.7	9.8	4	16	112
19087+0900		19:08:42.0	+09:00:05	SFR	22/01/99	0.263	74337	0.59	-63	13	9.3	21	74	103
19099+6711	U Dra	19:09:57.9	+67:11:36	STAR	25/01/00	0.263	79928	0.63	-80	80				111
19146+0959	IRC+10414	19:14:39.5	+09:59:17	STAR	25/01/00	0.263	79930	0.51	-115	95				110
19168+0814		19:16:51.1	+08:14:23	STAR	25/01/00	0.263	79932	0.52	-100	100				112
19175+0958		19:17:32.0	+09:58:35	STAR	19/01/00	0.263	79486	0.62	-55	160				112
19175+1042		19:17:34.9	+10:42:26	STAR	19/01/00	0.263	79488	0.59	-55	160				112
Source (1)	Other (2)	RA (1950) (3)	DEC (1950) (4)	Class (5)	Date (6)	ΔV (km s ⁻¹) (7)	Scan (8)	rms (Jy) (9)	V_{\min} (km s ⁻¹) (10)	V_{\max} (km s ⁻¹) (11)	V_{peak} (km s ⁻¹) (12)	F_p^{peak} (Jy) (13)	$\int F_\nu dV$ (Jy km s ⁻¹) (14)	Ref. ^(a) (15)
19184+1055		19:18:24.2	+10:55:14	STAR	19/01/00	0.263	79490	0.59	0	100				112
19206+2121		19:20:39.0	+21:21:05	STAR	19/01/00	0.263	79492	0.50	65	140				112
19214+0513		19:21:29.8	+05:13:07	STAR	19/01/00	0.263	79494	0.59	-100	100				112
19227+1700		19:22:45.6	+17:00:55	STAR	19/01/00	0.263	79496	0.68	-45	110				116
19229+1708		19:22:58.5	+17:08:49	STAR	19/01/00	0.263	79498	0.65	24.3	45.7	27.8	17	62	112
19248+1441		19:24:50.9	+14:41:16	STAR	19/01/00	0.263	79502	0.63	-60	100				112
19248+1122	IRC+10421	19:24:52.8	+11:22:55	STAR	18/01/00	0.263	79356	0.58	38.2	41.8	40.3	3	11	112
19258+1111		19:25:51.7	+11:11:17	STAR	18/01/00	0.263	79358	0.65	-100	100				112
19259+0510		19:25:54.0	+05:10:15	STAR	18/01/00	0.263	79360	0.65	-100	100				112
19268+1754		19:26:49.4	+17:54:54	SFR	14/03/97	0.263	56137	0.27	-85	131				104
					22/01/99	0.263	74339	1.17	-129	130				
19269+0813		19:26:57.0	+08:13:06	STAR	18/01/00	0.263	79362	0.59	-100	80				112
19270+2239		19:27:03.2	+22:39:30	STAR	18/01/00	0.263	79364	0.68	-100	100				117
19271+1354		19:27:11.9	+13:54:30	STAR	18/01/00	0.263	79366	0.58	50	58	52.0	6	19	112
19274+0919		19:27:27.7	+09:19:07	STAR	18/01/00	0.263	79368	0.80	-90	90				112
19276+1500		19:27:36.2	+15:00:28	STAR	18/01/00	0.263	79370	0.68	-70	100				112
19277+0947		19:27:44.9	+09:47:35	STAR	18/01/00	0.263	79372	0.85	-40	100				112
19291+0502		19:29:08.5	+05:02:11	STAR	18/01/00	0.263	79374	0.98	-100	80				112
19296+4331	UV Cyg	19:29:37.9	+43:31:45	STAR	18/01/00	0.263	79376	0.55	7.3	29	23.9	11	18	115
19305+2410		19:30:33.8	+24:10:24	STAR	18/01/00	0.263	79380	0.69	-80	80				112
19307+1338		19:30:42.8	+13:38:09	STAR	18/01/00	0.263	79382	1.02	37	44	41	14	21	117
19312+1130		19:31:13.2	+11:30:28	STAR	18/01/00	0.263	79384	1.11	-40	100				112
19316+0919		19:31:38.8	+09:19:30	STAR	25/01/00	0.263	79934	0.90	-15	110				112
19319+2214		19:31:54.8	+22:14:38	STAR	25/01/00	0.263	79936	0.90	-45	60				112
19321+2757	IRC+30374	19:32:08.8	+27:57:30	STAR	14/03/97	0.263	56139	0.94	-138	78				104
					22/01/99	0.263	74341	0.50	-185	73				
19325+1925		19:32:33.8	+19:25:04	SFR	14/03/97	0.263	56141	0.86	-120	97				104
					22/01/99	0.263	74343	0.52	-129	129				
19327+0903		19:32:46.7	+09:03:20	STAR	05/04/00	0.263	80382	1.38	38.9	44.5	42.4	8	11	112
19333+1918		19:33:18.7	+19:18:24	STAR	20/02/00	0.263	79940	0.76	-26.6	-24.9	-25.7	4	3	112
19338+2301		19:33:49.4	+23:01:43	UNKN	19/01/99	0.263	73930	0.54	1.9	4.8	3.4	4	4	104
19351+1922		19:35:08.3	+19:22:03	STAR	25/01/00	0.263	79942	0.85	-10	100				116
19352+1914		19:35:13.7	+19:14:03	STAR	25/01/00	0.263	79944	0.78	-100	30				112

distributed in the upper part of the plane. The box in the upper right corresponds to the color criteria adopted by Wood & Churchwell (1989) to identify ultracompact HII regions. The majority of the SFR-type sources are lo-

cated within these boundaries, consistent with the idea that H₂O masers are active preferentially during the earliest phases of the evolution of bright, massive stars.

Table 1. continued

Source (1)	Other (2)	RA (1950) (3)	DEC (1950) (4)	Class (5)	Date (6)	ΔV (km s ⁻¹) (7)	Scan (8)	rms (Jy) (9)	V_{\min} (km s ⁻¹) (10)	V_{\max} (km s ⁻¹) (11)	V_{peak} (km s ⁻¹) (12)	F_{ν}^{peak} (Jy) (13)	$\int F_{\nu} dV$ (Jy km s ⁻¹) (14)	Ref. ^(a) (15)
19361–1658	AFGL 2425	19:36:09.0	-16:58:50	STAR	18/01/00	0.263	79354	0.98	58.8	62.8	61.7	6	16	111
	BG Cyg	19:36:36.9	+28:23:51		25/01/00	0.263	79946	0.78	-100	15				111
19366+1149	SV Aql	19:36:40.8	+11:49:50	STAR	25/01/00	0.263	79948	0.80	-52.3	-49.1	-50.4	4	4	112
19368+2239		19:36:49.7	+22:39:37	SFR	31/03/99	0.263	75214	0.79	32.2	40.5	36.6	7	8	120
19371+2855		19:37:07.3	+28:55:41	STAR	25/01/00	0.263	79950	0.83	-100	100				112
19374+2359		19:37:28.7	+23:59:27	STAR	14/03/97	0.263	56145	0.82	-148	68				104
					22/01/99	0.263	74345	0.50	-194	64				
19378+1256	V455 Aql	19:37:53.4	+12:56:08	STAR	25/01/00	0.263	79952	0.84	-160	10				112
19382+3400		19:38:14.8	+34:00:15	STAR	25/01/00	0.263	79954	0.81	-100	35				112
19394+4840	V391 Cyg	19:39:26.0	+48:40:26	STAR	25/01/00	0.263	79956	0.77	-25	-20	-22.5	76	83	111
19399+2258		19:39:54.9	+22:58:55	STAR	25/01/00	0.263	79958	0.84	-100	100				116,117
19412+0337	IRC+00450	19:41:15.3	+03:37:15	STAR	25/01/00	0.263	79960	1.20	-41.3	-35.9	-39.0	13	46	112
19425+3323		19:42:35.3	+33:23:17	STAR	25/01/00	0.263	79962	0.87	-100	100				112
19437+2408		19:43:46.3	+24:08:10	UNKN	25/01/00	0.263	79964	0.91	-100	100				117
19451+1628		19:45:10.5	+16:28:05	STAR	25/01/00	0.263	79966	1.27	-100	100				112
19453+1917		19:45:22.1	+19:17:20	STAR	25/01/00	0.263	79968	1.17	-70	90				112
19454+2536		19:45:25.5	+25:36:01	STAR	25/01/00	0.263	79970	1.14	-60	160				112
19454+0355		19:45:25.9	+03:55:04	STAR	26/01/00	0.263	80044	1.50	-80	100				117
19455+0920		19:45:32.3	+09:20:40	STAR	14/03/97	0.263	56147	0.83	-81	136				104
					21/01/99	0.263	74195	0.63	-128	130				
19466+2751		19:46:35.9	+27:51:59	STAR	26/01/00	0.263	80046	0.70	-2.8	5.0	3.3	15	33	116
19471+2641		19:47:06.1	+26:41:16	SFR	14/03/97	0.263	56149	0.77	21.1	37.5	23.8	11	27	104
					21/01/99	0.263	74197	0.53	-160	50				
19471+2944		19:47:10.8	+29:44:56	STAR	26/01/00	0.263	80048	0.70	-100	0				112
19479+2111		19:47:56.5	+21:11:24	STAR	26/01/00	0.263	80050	0.77	-55	95				112
19516+2217		19:51:40.1	+22:17:46	STAR	26/01/00	0.263	80054	0.80	-60	80				112
19519+2527		19:51:57.5	+25:27:10	STAR	26/01/00	0.263	80056	0.78	-19	-13	-16	10	24	117
19522+2653		19:52:12.7	+26:53:43	STAR	26/01/00	0.263	80058	0.79	-100	0				112
19535+2157		19:53:31.5	+21:57:29	STAR	26/01/00	0.263	80060	0.76	-55	100				112
19547+1848	RX Sge	19:54:42.5	+18:48:00	STAR	26/01/00	0.263	80062	0.74	-50	100				112
19560+3135		19:56:05.5	+31:35:57	SFR	31/03/99	0.263	75224	0.77	-74.4	-63.5	-70.9	7	29	120
19564–0801	RS Aql	19:56:24.5	-08:01:15	STAR	27/12/99	0.263	79002	0.98	-100	120				111
19565+3140		19:56:32.0	+31:40:00	STAR	27/12/99	0.263	79004	0.53	-110	110				112

Source (1)	Other (2)	RA (1950) (3)	DEC (1950) (4)	Class (5)	Date (6)	ΔV (km s ⁻¹) (7)	Scan (8)	rms (Jy) (9)	V_{\min} (km s ⁻¹) (10)	V_{\max} (km s ⁻¹) (11)	V_{peak} (km s ⁻¹) (12)	F_{ν}^{peak} (Jy) (13)	$\int F_{\nu} dV$ (Jy km s ⁻¹) (14)	Ref. ^(a) (15)
19573+2204		19:57:19.1	+22:04:49	STAR	27/12/99	0.263	79006	0.49	-120	110				112
19575+1143		19:57:34.4	+11:43:27	STAR	27/12/99	0.263	79008	0.55	-100	100				112
19579+3223		19:57:54.0	+32:23:50	STAR	27/12/99	0.263	79010	0.51	0	22	16.6	3	17	112
19579+2926		19:57:54.3	+29:26:13	STAR	17/01/00	0.263	79221	3.65	-100	100				112
19589+3320		19:58:57.0	+33:20:47	SFR	14/03/97	0.263	56151	0.84	-136	81				104
					21/01/99	0.263	74199	0.52	-182	75				
19592+3302		19:59:13.7	+33:02:47	SFR	19/01/94	0.164	32903	1.12	-148	20				104
					14/03/97	0.263	56175	0.24	-70	147				
					21/01/99	0.263	74201	0.51	-130	129				
20010+3011		20:01:05.2	+30:11:45	STAR	14/03/97	0.263	56177	1.14	17.8	26.5	22.6	12	17	104
					20/01/99	0.263	74057	0.40	16.3	25.6	18.6	4	14	
20011+1752	G57.27–6.92	20:01:10.4	+17:52:02	STAR	17/01/00	0.263	79223	1.02	-100	100				112
20015+3019	V719 Cyg	20:01:34.9	+30:19:24	STAR	17/01/00	0.263	79225	0.8	14	28	16.4	19	75	112
20024+1727		20:02:24.6	+17:27:22	STAR	17/01/00	0.263	79227	0.65	-100	100				112
20028+3910		20:02:48.0	+39:10:03	STAR	14/03/97	0.263	56179	0.33	-93	123				104
					20/01/99	0.263	74059	0.52	-141	119				
20072+3116		20:07:15.0	+31:16:52	STAR	19/01/99	0.263	73932	0.75	-80	179				104
20109+3205	V557 Cyg	20:10:57.9	+32:05:39	STAR	05/04/00	0.263	80384	1.07	51.1	55.3	53.3	8	12	111
20115+0844		20:11:33.0	+08:44:14	STAR	17/01/00	0.263	79233	0.70	-100	120				112
20125+0856	R Del	20:12:29.9	+08:56:08	STAR	17/01/00	0.263	79235	0.78	-35.3	-27.8	-31.5	71	61	111,114
20140+3620		20:14:01.4	+36:20:48	STAR	17/01/00	0.263	79237	0.67	-100	100				112
20153+2057		20:15:23.5	+20:57:45	STAR	17/01/00	0.263	79239	0.60	-100	120				112
20160+0725		20:16:02.4	+07:25:40	STAR	17/01/00	0.263	79241	0.93	-90	130				117
20216+4107		20:21:37.4	+41:07:56	SFR	19/01/94	0.165	32951	0.86	-86	83				104
					14/03/97	0.263	56181	1.06	-137	78				
					20/01/99	0.263	74063	0.53	-186	73				
20248+7505	UU Dra	20:24:53.8	+75:05:24	STAR	17/01/00	0.263	79245	0.96	-120	100				115
20280+2631		20:28:00.7	+26:31:25	STAR	17/01/00	0.263	79247	0.67	-90	120				112
20300+3847		20:30:01.4	+38:47:09	SFR	14/03/97	0.263	56183	1.04	-144	73				104
					20/01/99	0.263	74065	0.52	-192	68				

The Medicina radiotelescope has been extensively used for water maser searches. In Fig. 5 we show the distribution of the 5074 independent positions in our database, using the same criterion of considering two positions in-

dependent if separated by more than 1 arcmin. The total sky coverage is small, with a noticeable higher coverage toward the galactic plane. Of the 5074 centers observed with the Medicina antenna, 1013 are known to be

Table 1. continued

Source (1)	Other (2)	RA (1950) (3)	DEC (1950) (4)	Class (5)	Date (6)	ΔV (km s ⁻¹) (7)	Scan (8)	rms (Jy) (9)	V_{\min} (km s ⁻¹) (10)	V_{\max} (km s ⁻¹) (11)	V_{peak} (km s ⁻¹) (12)	F_{ν}^{peak} (Jy) (13)	$\int F_{\nu} dV$ (Jy km s ⁻¹) (14)	Ref. ^(a) (15)
20306+3749		20:30:41.8	+37:49:20	SFR	19/03/99	0.263	74914	0.89	-94.3	-78.2	-89.1	37	171	120
20311+4222		20:31:09.3	+42:22:39	STAR	14/03/97	0.263	56185	1.04	-81	135				104
					20/01/99	0.263	74067	0.11	-128	130				
20350+4126		20:35:04.4	+41:26:02	SFR	22/04/93	0.329	28364	0.97	-168	167				104
					14/03/97	0.263	56187	1.03	-86	131				
					20/01/99	0.263	74069	0.45	-129	129				
20351+3450		20:35:09.9	+34:50:37	STAR	17/01/00	0.263	79249	0.70	-100	120				112
20386+6751	L1157	20:38:39.3	+67:51:36	SFR	13/03/97	0.263	56063	1.24	-146	70				104,109
					07/05/97	0.263	59283	0.88	-145	69				
					01/07/97	0.263	60663	1.03	-160	109				
					08/04/98	0.132	70955	1.52	-40	67				
					20/01/99	0.263	74071	0.31	-154	105				
20396+4757		20:39:41.8	+47:57:45	STAR	14/03/97	0.263	56189	1.06	-60	156				104
					20/01/99	0.263	74075	0.52	-107	151				
20403+3700		20:40:23.3	+37:00:51	STAR	17/01/00	0.263	79252	0.72	-63.6	-56.2	-59.3	6	9	112
20406+2953		20:40:41.5	+29:53:18	STRN	14/03/97	0.263	56191	1.50	-111	106				104
					20/01/99	0.263	74077	0.51	-158	100				
20417+3759	DR Cyg	20:41:46.9	+37:59:02	STAR	05/04/00	0.263	80386	1.11	11.7	14.0	12.9	100	74	111
21027+5309		21:02:43.4	+53:09:04	STAR	14/03/97	0.263	56193	0.69	-140	77				104
					20/01/99	0.263	74079	0.47	-187	72				
21086+5238	IRC+50362	21:08:39.2	+52:38:44	STAR	24/01/00	0.263	79824	0.61	-13.5	-8.3	-11.4	3	6	110
21088+6817	T Cep	21:08:51.9	+68:17:24	STAR	13/03/97	0.263	56065	1.28	-101	115				104
					21/01/99	0.263	74205	0.46	-148	110				
21106+4712		21:10:36.0	+47:12:01	SFR	19/01/99	0.263	73936	0.73	-130	129				107
21115+5953		21:11:30.6	+59:53:24	STAR	13/03/97	0.263	56067	2.42	-112	103				104
					21/01/99	0.263	74207	0.51	-161	98				
21208+7737	GH Cep	21:20:42.0	+77:37:47	STAR	24/01/00	0.263	79826	0.54	34.6	37.2	35.9	3	7	111
21305+2118		21:30:33.0	+21:18:23	STAR	07/05/97	0.263	59289	0.91	-119	98				104
					21/01/99	0.263	74209	0.49	-166	93				
21358+7823	S Cep	21:35:52.2	+78:23:59	STAR	13/03/97	0.263	56069	1.05	-159	57				104
					21/01/99	0.263	74211	0.39	-207	52				

Source (1)	Other (2)	RA (1950) (3)	DEC (1950) (4)	Class (5)	Date (6)	ΔV (km s ⁻¹) (7)	Scan (8)	rms (Jy) (9)	V_{\min} (km s ⁻¹) (10)	V_{\max} (km s ⁻¹) (11)	V_{peak} (km s ⁻¹) (12)	F_{ν}^{peak} (Jy) (13)	$\int F_{\nu} dV$ (Jy km s ⁻¹) (14)	Ref. ^(a) (15)
21419+5833	MU Cep	21:41:58.0	+58:33:03	STAR	24/01/00	0.263	79828	0.58	-80	130				113,114
21426+1228	TU Peg	21:42:39.0	+12:28:00	STAR	24/01/00	0.263	79830	0.62	8.0	13.5	10.3	8	13	111
21576+3259	WX Peg	21:57:37.3	+32:59:23	STAR	24/01/00	0.263	79832	0.53	-140	60				112
22097+5647	CU Cep	22:09:44.9	+56:47:27	STAR	27/12/99	0.263	79012	0.59	-160	60				111
22180+3225	YZ Peg	22:18:05.6	+32:25:32	STAR	27/12/99	0.263	79014	0.57	-130	110				112
22241+6005		22:24:07.1	+60:05:31	STAR	13/03/97	0.263	56071	2.06	-111	105				104
					20/01/99	0.263	74087	0.51	-158	99				
22267+6244		22:26:46.7	+62:44:22	SFR	19/03/99	0.263	74924	0.64	-2.0	5.9	1.5	5	6	120
22343+7501	L1251 A	22:34:21.9	+75:01:32	SFR	20/01/99	0.263	74089	0.45	-13.3	-9.3	-11.2	24	21	100,107,108
					05/04/00	0.263	80388	1.08	-105	90				
22376+7455		22:37:36.0	+74:55:00	SFR	19/01/99	0.263	73940	0.56	-125	133	2.1	9	22	106
22453+6146	L1211	22:45:23.2	+61:46:07	SFR	13/03/97	0.263	56073	1.93	-95	122				104
					20/01/99	0.263	74093	0.46	-142	117				
22480+6002		22:48:00.9	+60:02:01	STAR	13/03/97	0.263	56075	2.12	-53.2	-42.3	-50.2	48	110	120
					20/01/99	0.263	74095	0.59	-60.7	-43.3	-50.3	160	290	
22510+3614	IRC+40525	22:51:00.0	+36:14:26	STAR	27/12/99	0.263	79016	0.65	-170	10				112
22512+6100		22:51:13.6	+61:00:58	STAR	13/03/97	0.263	56077	2.23	-52.3	-47.3	-49.2	17	34	104
					20/01/99	0.263	74113	0.54	-136	123				
22542+5815		22:54:13.5	+58:15:11	SFR	20/01/99	0.263	74099	0.44	-168	91				104
22551+6140		22:55:11.6	+61:40:00	SFR	13/03/97	0.263	56081	1.71	-117	100				104
					20/01/99	0.263	74101	0.53	-165	93				
22553+1744	BI Peg	22:55:23.6	+17:44:58	STAR	24/01/00	0.263	79834	0.50	-100	35				115
23140+6121		23:14:01.8	+61:21:22	SFR	14/03/97	0.263	56083	1.64	-70	147				104
					20/01/99	0.263	74107	0.73	-48.3	-44.5	-47.0	5	4	
	G108.38-8.71	23:15:05.4	+51:12:41	STAR	19/01/99	0.263	73942	0.69	-182	77				102
23166+1655	AFGL3068	23:16:41.7	+16:55:10	STAR	07/05/97	0.263	56291	1.00	-135	81				104
					20/01/99	0.263	74109	0.96	-183	76				
23279+5336		23:27:56.3	+53:36:34	STAR	07/05/97	0.263	56293	1.32	-104	112				104
					20/01/99	0.263	74111	0.63	-152	107				
23545+6508		23:54:34.0	+65:08:29	SFR	31/03/99	0.263	75236	0.70	-29.9	-23.1	-27.3	4	3	120
23561+6609	LkH0259	23:56:09.6	+66:09:32	SFR	14/03/97	0.263	56085	1.49	-165	51				104

^(a) The reference codes are as follows: 100 Xiang & Turner (1995); 101 Codella & Palla (1995); 102 Miralles et al. (1994); 103 Codella et al. (1995); 104 Han et al. (1995); 105 Codella et al. (1996); 106 Toth & Kun (1997); 107 Glaussen et al. (1996); 108 Toth & Walmsley (1994); 109 Meehan et al. (1998); 110 Lewis (1997); 111 Benson & Little-Marein (1996); 112 Engels & Lewis (1996); 113 Takaba (1994); 114 Benson et al. (1990); 115 Szymczak & Engels (1995); 116 Lewis & Engels (1993); 117 Lewis & Engels (1995); 118 Szymczak & Engels (1997); 119 Codella & Moscadelli (2000); 120 Present Work.

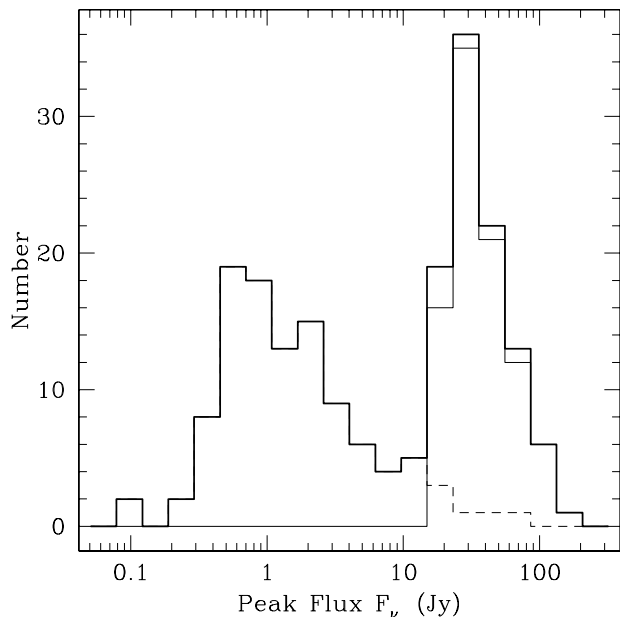


Fig. 2. The distribution (thick histogram) of the peak H₂O fluxes taken from the literature for the sources not detected in our survey. The thin solid line represents the distribution of the peak fluxes published by Han et al. (1995). The dashed curve is the difference of the thick and thin histograms. At peak fluxes lower than ~ 15 Jy, this curve coincides with the thick histogram

associated with H₂O maser emission. This corresponds to a high fraction (20%), which is simply the result of the biased searches conducted with the Medicina antenna: in fact, the large majority of the observations were carried out towards known H₂O masers taken from the literature and/or associated with IRAS point sources, which are expected to show maser emission.

In Fig. 6 we show the distributions of the masers of type SFR (top) and those of type STAR (bottom). The two distributions are clearly different, with SFR concentrated towards the galactic plane and STAR much more uniformly distributed in galactic latitude. Such distributions are consistent with those expected respectively for young stars and late-type stars, thus giving further support to our classification based on color indices.

In Fig. 7 we show the distribution of the H₂O integrated fluxes for the 423 maser sources detected by Comoretto et al. (1990), U1, and U2. The percentage of very bright masers is very small compared to the total. While the slope of the right part of the distribution represents the true increase in the number of sources towards lower integrated fluxes, the peak and subsequent decrease are instrumental effects due to the sensitivity limit. In order to inspect whether the brightest masers have all been detected in the first catalogs, we show in the lower panel of Fig. 7 the 203 sources detected by Comoretto et al. (1990) (full histogram), the 137 detected by U1 (dotted), and the 83 detected by U2 (dashed). The indication that emerges from this comparison is that continuing searches of new water masers tend to populate the region of lower

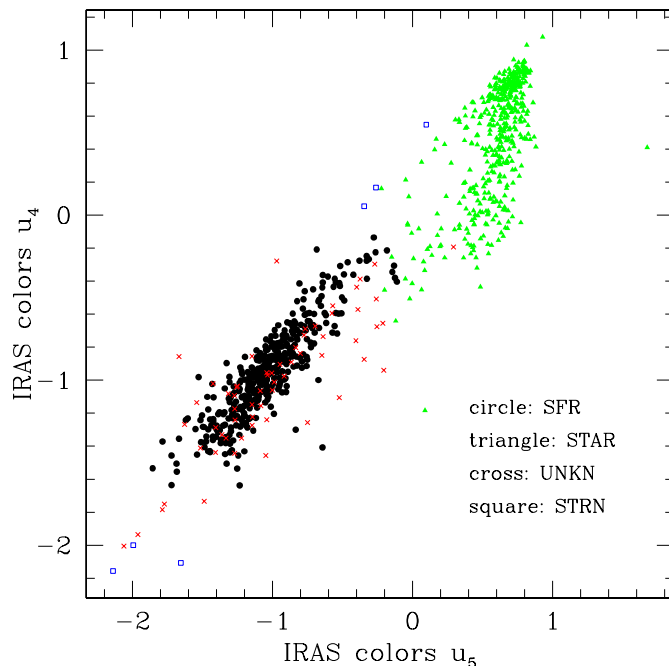


Fig. 3. The distribution in the u_4 vs. u_5 plane of the 937 sources of the Arcetri Catalog with an IRAS PSC counterpart. Water masers associated with SFR and STAR are clearly separated in this diagram

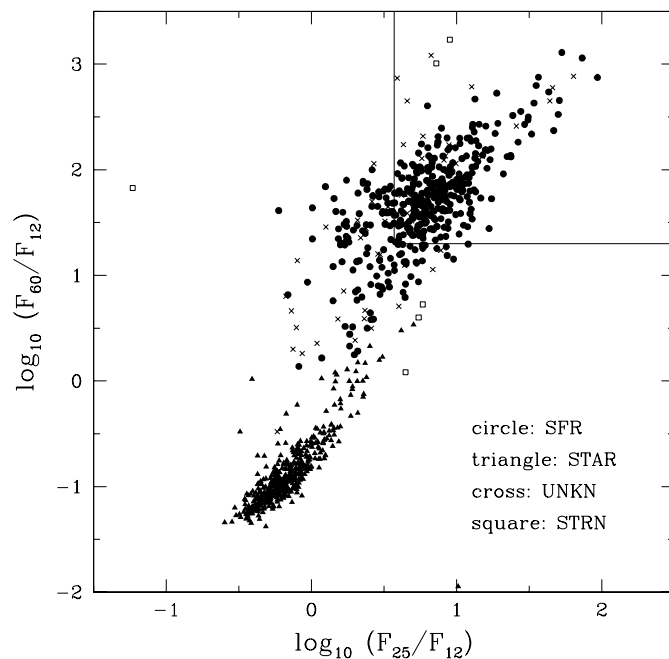


Fig. 4. Distribution in the $[60-12]$, $[25-12]$ plane of the 937 sources of the Arcetri Catalog with IRAS counterpart. The symbols have the same meaning as in Fig. 3. The box in the upper right corner delimits the colors for ultracompact HII regions, as suggested by Wood & Churchwell (1989)

integrated fluxes and that very few masers with integrated fluxes above $1000 \text{ Jy km s}^{-1}$ have been detected in more recent surveys.

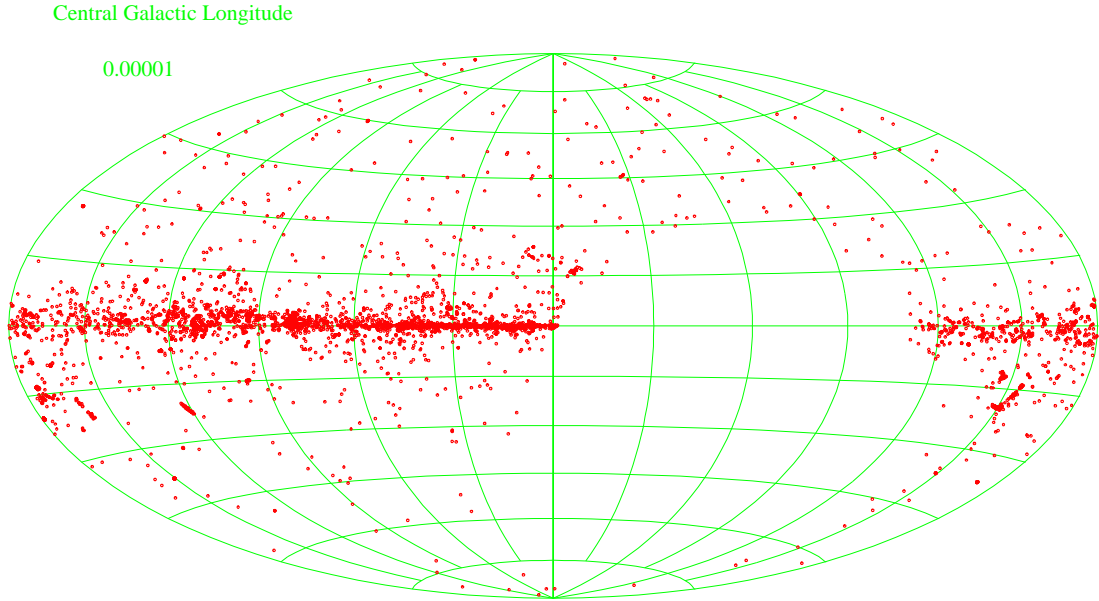


Fig. 5. Distribution in galactic coordinates of the 5074 positions observed at the frequency of the 22 GHz H₂O maser line with the Medicina antenna since 1987

Finally, Fig. 8 shows the distribution of the integrated fluxes of maser sources detected by Comoretto et al. (1990), U1, and U2, separated into SFR (255) and STAR (133). Clearly, both distributions peak at the same integrated flux, but the SFR distribution is broader towards higher values. This indicates that H₂O masers associated with late-type stars are likely to be fainter than those found in star forming regions.

Acknowledgements. The technical staff at the Medicina station is gratefully acknowledged for the competent and constant assistance during all the observing runs. We also thank the referee for a very useful report which resulted in a substantial improvement of the paper.

Appendix A: Classification scheme of the sources with IRAS counterparts

Palagi et al. (1993) describe a procedure which classifies the H₂O maser sources into two classes: those arising in star forming regions (SFR) and those found around late-type stars (STAR), according to the four FIR fluxes of the IRAS point source associated to the maser.

The classification criteria are derived applying a multivariate analysis (principal component analysis and linear discriminant analysis, Murtagh & Heck 1987) to the subsample of the Arcetri H₂O maser catalog that satisfies the following conditions:

- the H₂O maser source has a good morphological classification as SFR or STAR.
- the associated IRAS point source has no upper limit in any of the four bands.

Table A.1. Boundary definition of SFR and STAR regions

	STAR	SFR
u_1	+0.1 to +1.4	-2.4 to -0.3
u_2	-1.8 to +0.8	-1.2 to +1.2
u_3	-1.4 to +0.5	-1.0 to +1.3
u_4	+0.0 to +1.2	-2.0 to -0.1
u_5	-0.2 to +1.0	-3.6 to -0.4

The results of the multivariate analysis can be summarized as follows:

- the principal component analysis provides three new observables u_1 (Eq. A1), u_2 (Eq. A2) and u_3 (Eq. A3) as combinations of the logarithms of the IRAS fluxes, whose distributions show that the subsample is composed of two main populations well correlated with the morphological classification of the H₂O masers;
- the linear discriminant analysis provides a fourth combination of the IRAS colors, u_4 (Eq. A4), which maximizes the separation of the two populations;
- since a relevant fraction of the IRAS sources associated with the H₂O masers have an upper limit at $\lambda = 100 \mu\text{m}$ we derived a combination of IRAS colors, $u_5 = u_4 - 0.480 \cdot u_2$ (Eq. A5), that is independent of the $100 \mu\text{m}$ flux, but preserves most of the discriminating properties of u_4 ;
- from the distributions of each IRAS color combination we derive the boundaries of the STAR and SFR classes, as reported in Table A.1.

The five combinations of the logarithms of the FIR fluxes determined through the multivariate analysis are:

$$u_1 = +0.510[f_{12}] - 0.137[f_{25}] + 0.403[f_{60}] - 0.776[f_{100}] \quad (\text{A.1})$$

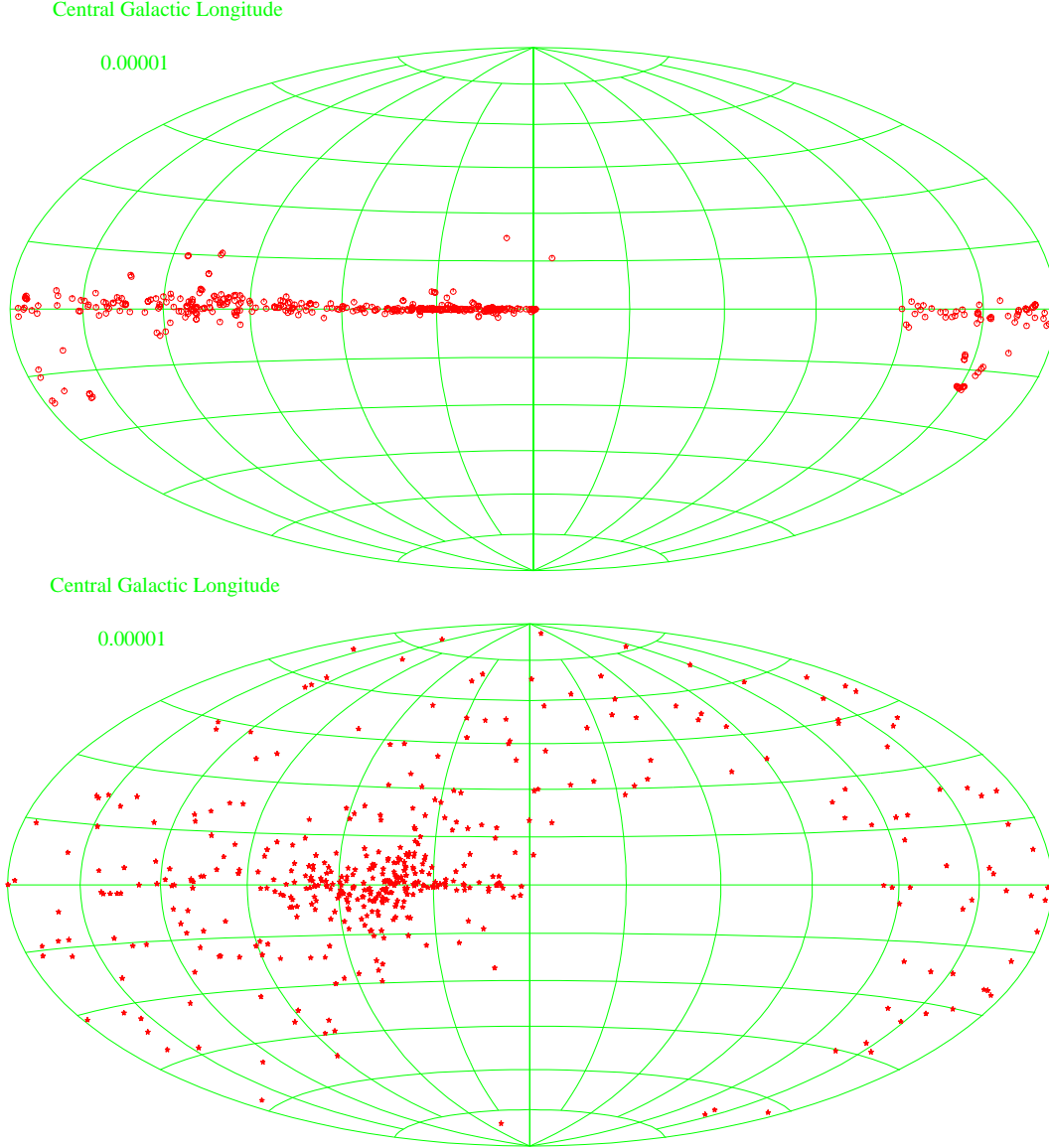


Fig. 6. Distributions in galactic coordinates of the H₂O maser centers observed in the surveys of Comoretto et al. (1990), U1, and U2. The top panel shows the 410 sources classified as SFR and the bottom the 460 classified as STAR

Table A.2. Classification criteria

u_4	Color quality			u_5
	Good	Upper	Lower	
$u_4 < -2.0$	STRN	STRN	UNKN	$u_5 < -3.6$
$-2.0 < u_4 < -0.1$	SFR	SFR	UNKN	$-3.6 < u_5 < -0.4$
$-0.1 < u_4 < 0.0$	UNKN	UNKN	UNKN	$-0.4 < u_5 < -0.2$
$0.0 < u_4 < +1.2$	STAR	UNKN	STAR	$-0.2 < u_5 < +1.0$
$u_4 > +1.2$	STRN	UNKN	STRN	$u_5 > +1.0$

$$u_2 = -0.533[f_{12}] + 0.522[f_{25}] + 0.857[f_{60}] - 0.846[f_{100}] \quad (\text{A.2})$$

$$u_3 = +0.473[f_{12}] - 1.057[f_{25}] + 1.244[f_{60}] - 0.660[f_{100}] \quad (\text{A.3})$$

$$u_4 = +0.226[f_{12}] + 0.501[f_{25}] - 0.324[f_{60}] - 0.403[f_{100}] \quad (\text{A.4})$$

$$u_5 = +0.482[f_{12}] + 0.250[f_{25}] - 0.735[f_{60}] \quad (\text{A.5})$$

where $[f_u] = \log_{10}(f_u)$, with $u = 12, 25, 60, 100$. Based on the criteria determined from this subset of the Arcetri Catalog, for the remainder of the sources the classification proceeds as follows (see Fig. A.1 for the flow-chart representation):

1. If there are no upper limits in flux density, u_4 is considered a Good value and is compared with the class boundaries of Table A.1. The outcome is given by the

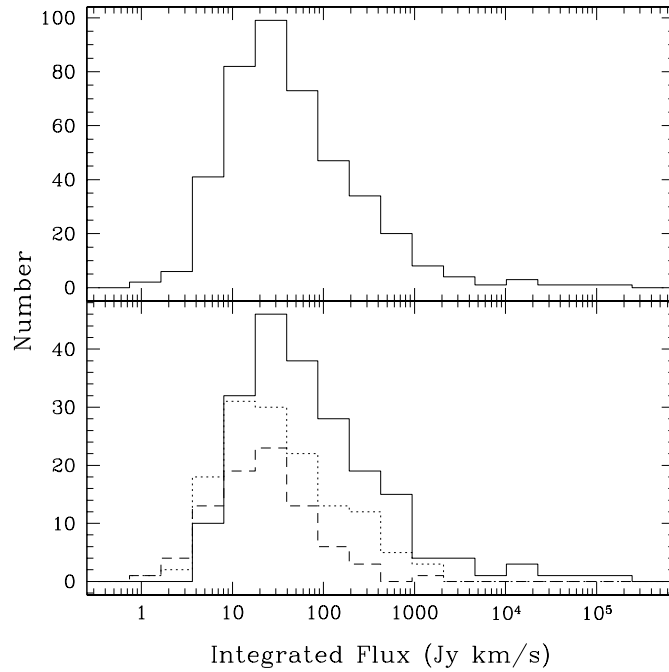


Fig. 7. Distributions of the integrated flux of the 423 maser sources detected by Comoretto et al. (1990), U1, and U2. The top panel shows the global distribution, while in the bottom panel a distinction is made between the 203 sources detected by Comoretto et al. (1990) (full histogram), the 137 detected by U1 (dotted), and the 83 detected by U2 (dashed)

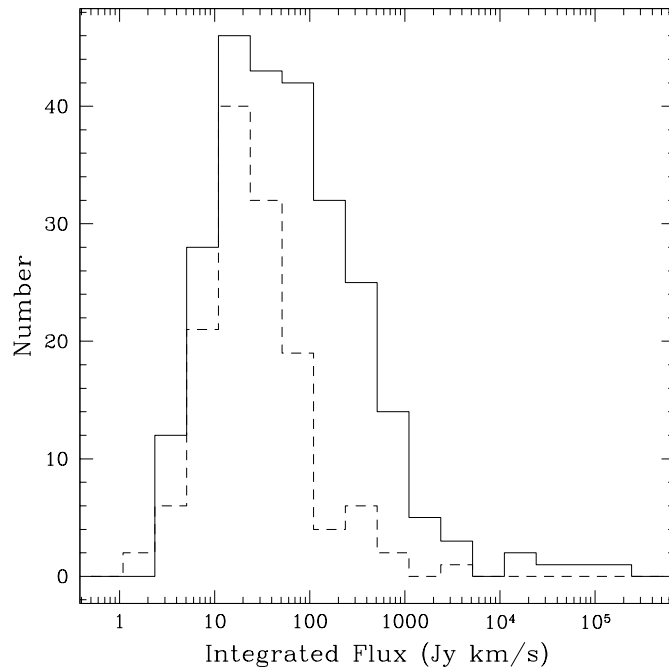


Fig. 8. Distributions of the integrated flux of maser sources detected by Comoretto et al. (1990), U1, and U2, according to their classification: 255 SFR (full histogram) and 133 STAR (dashed)

- Good column of Table A.2, where UNKN stands for *unknown* and STRN stands for *strange*;
2. If the combination of upper limits in the FIR fluxes is such that u_4 can be assigned an Upper or Lower limit, then the corresponding column of Table A.2 gives the outcome of the classification;
 3. If the outcome of the classification based on u_4 is UNKN, u_5 is computed and the procedure is iterated once more starting from point 2 and using the appropriate class boundaries;
 4. In any case, when the outcome is either SFR or STAR, it is checked against u_2 and u_3 for consistency. If the check is not passed, the source is classified as STRN.

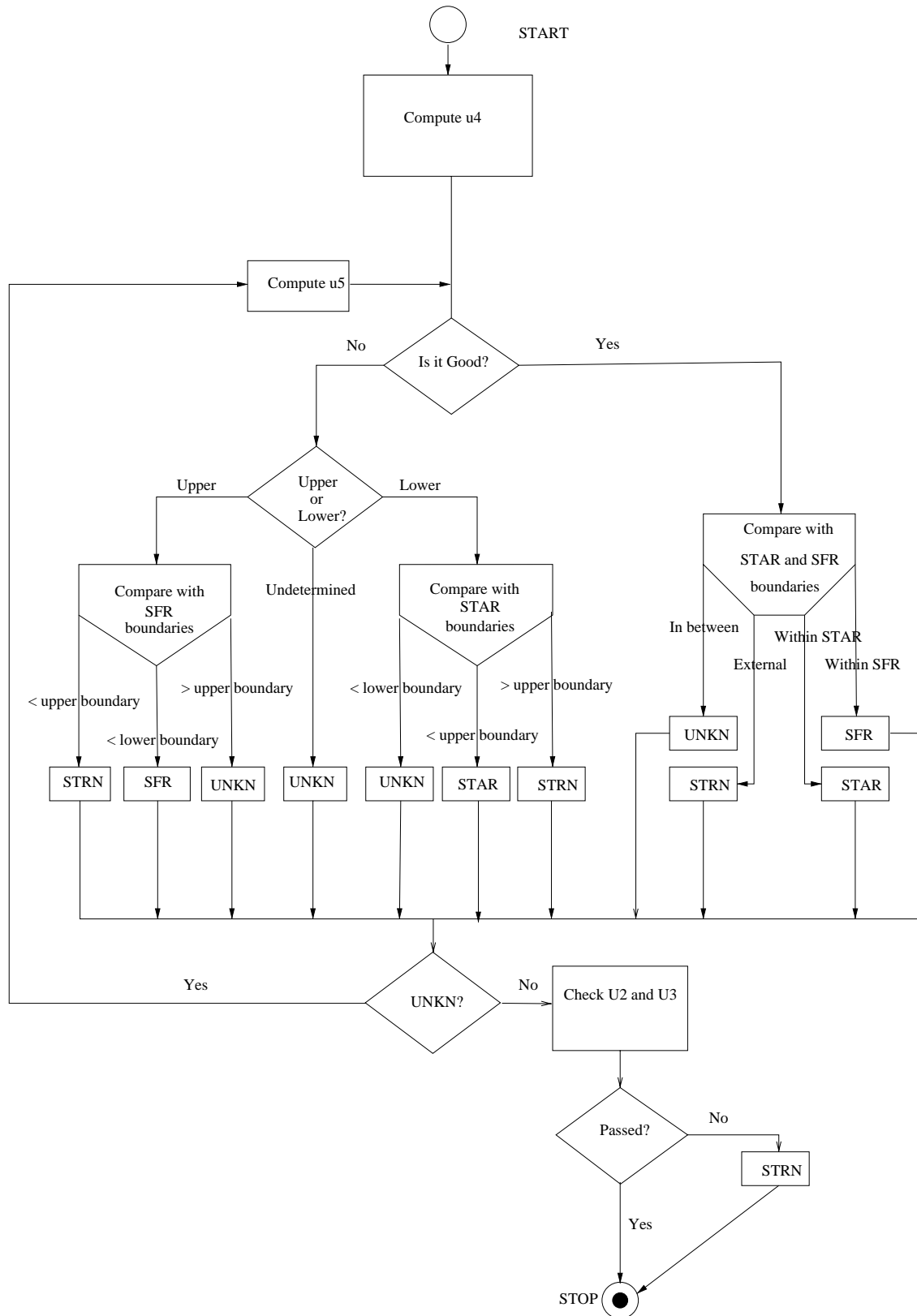


Fig. A.1. Flowchart of the classification procedure

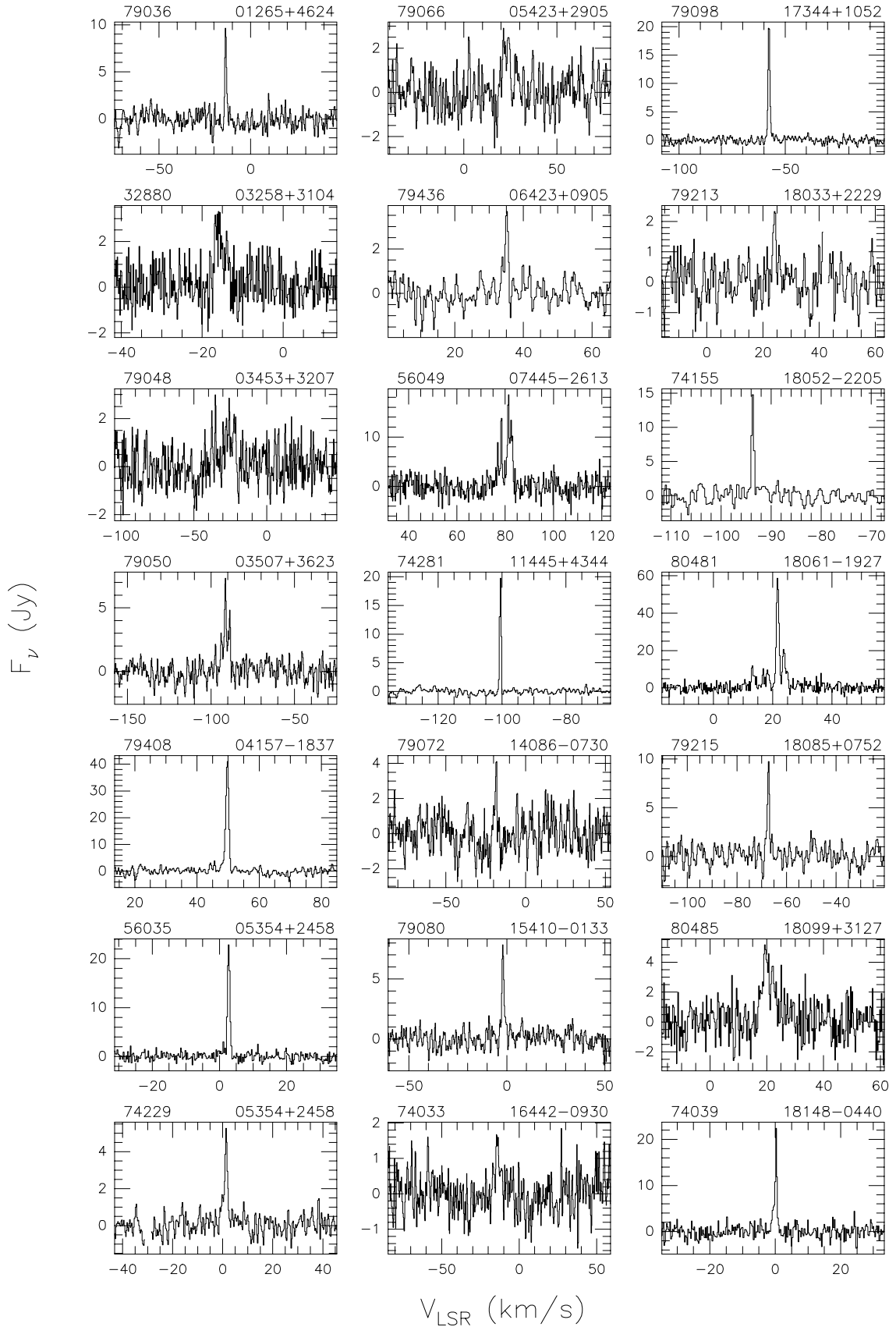


Fig. A.2. Spectra of all the detections listed in Table 1. Each source is identified by the scan number (upper left) and source name (upper right). The spectra are ordered in right ascension from top left to bottom right

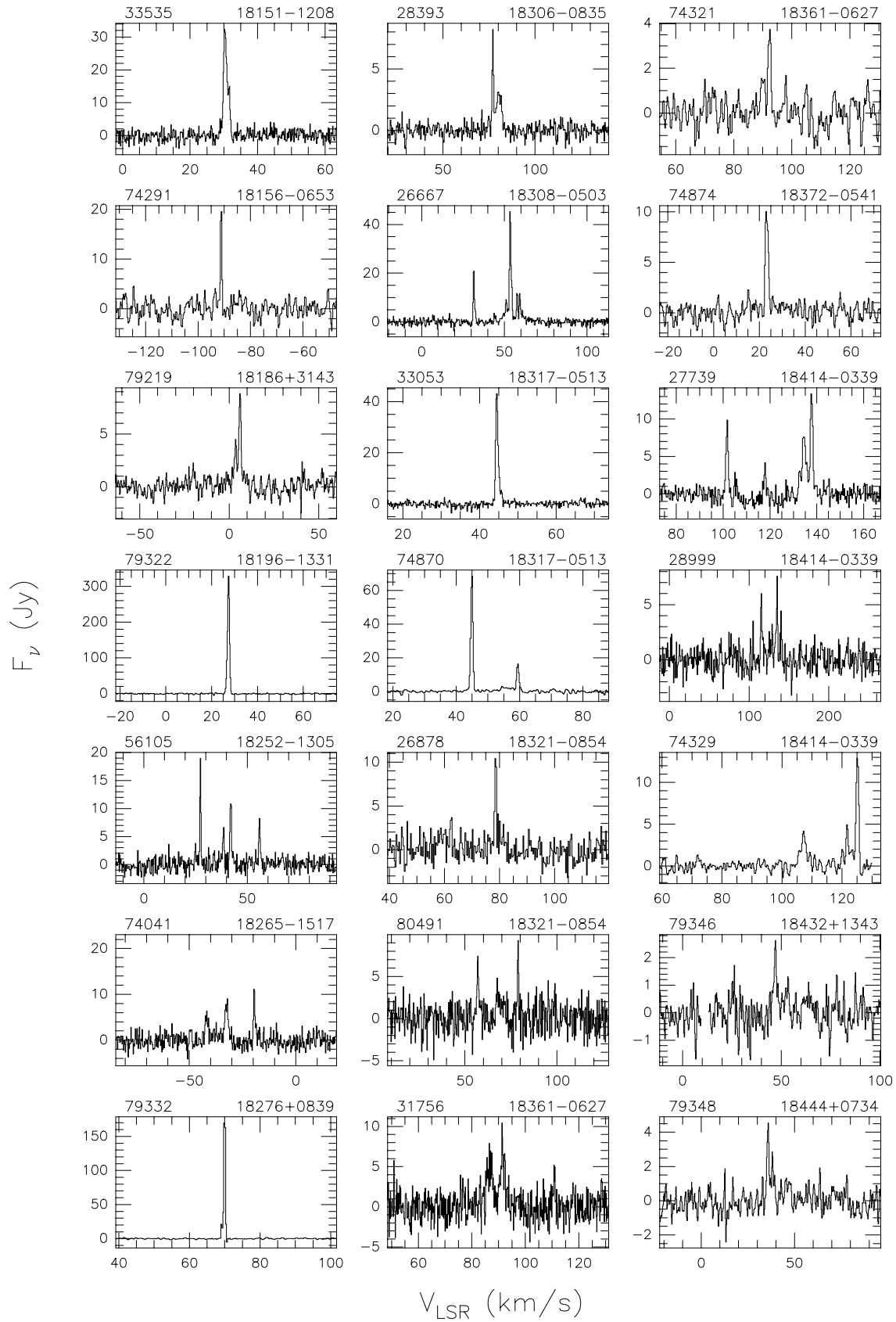


Fig. A.2. continued

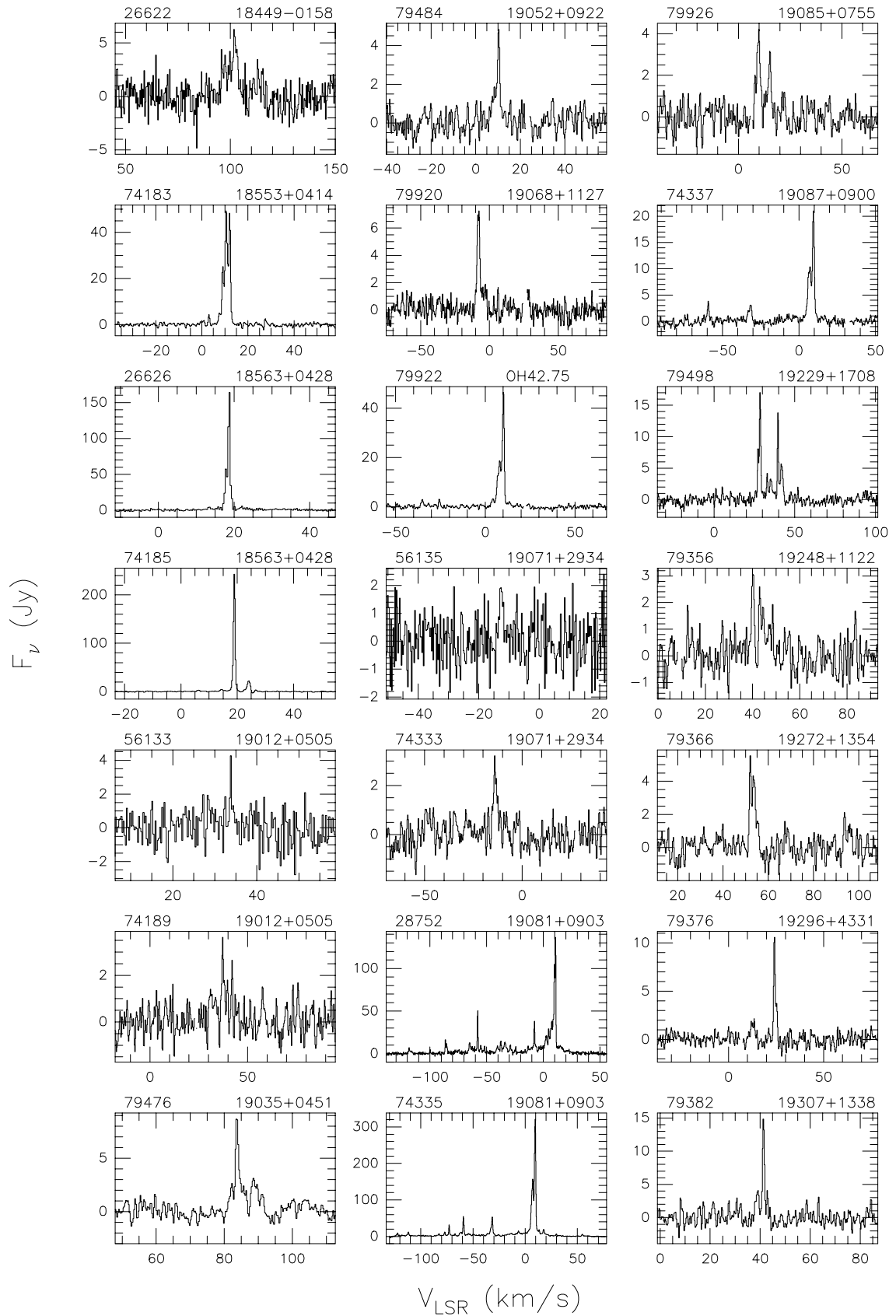


Fig. A.2. continued

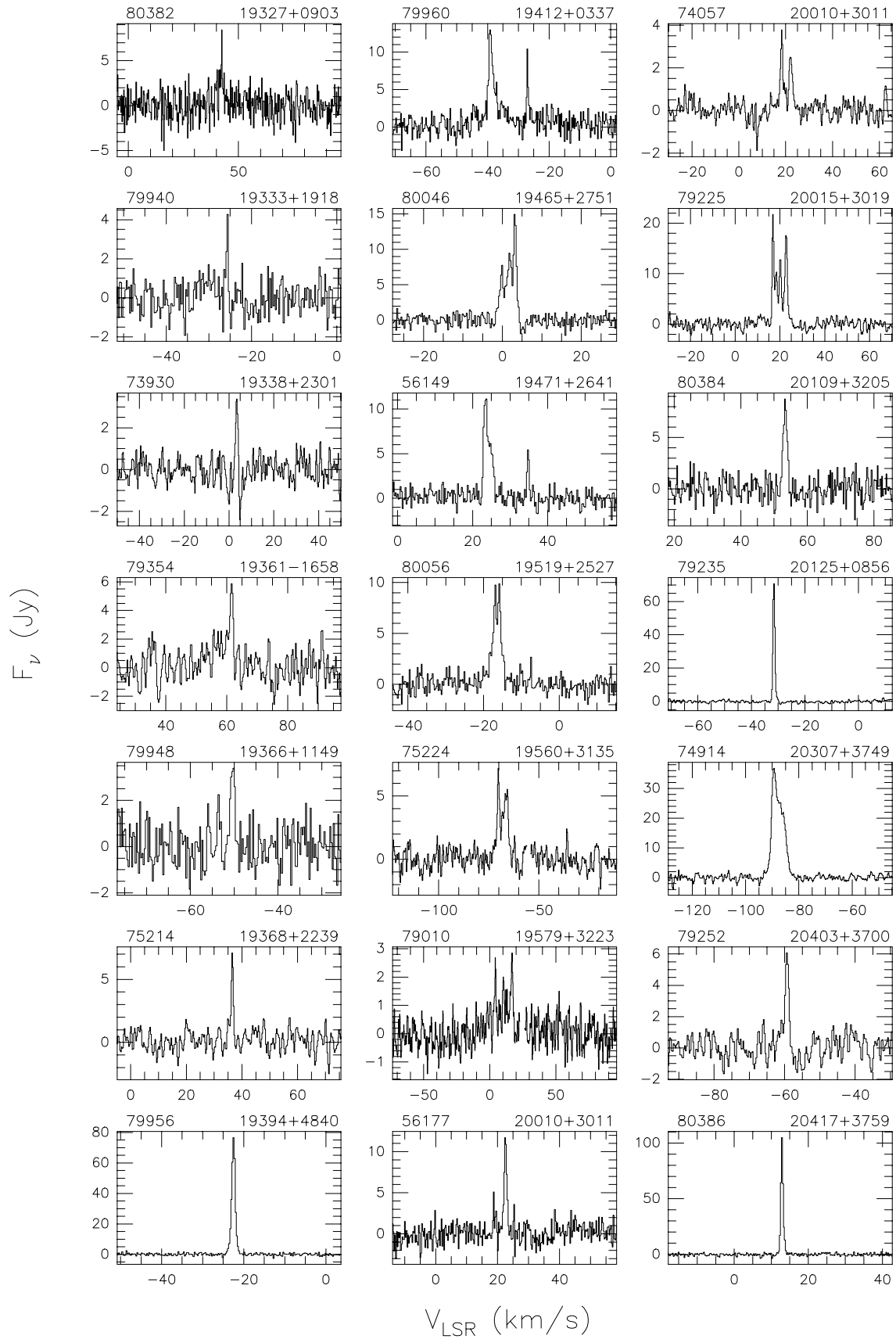


Fig. A.2. continued

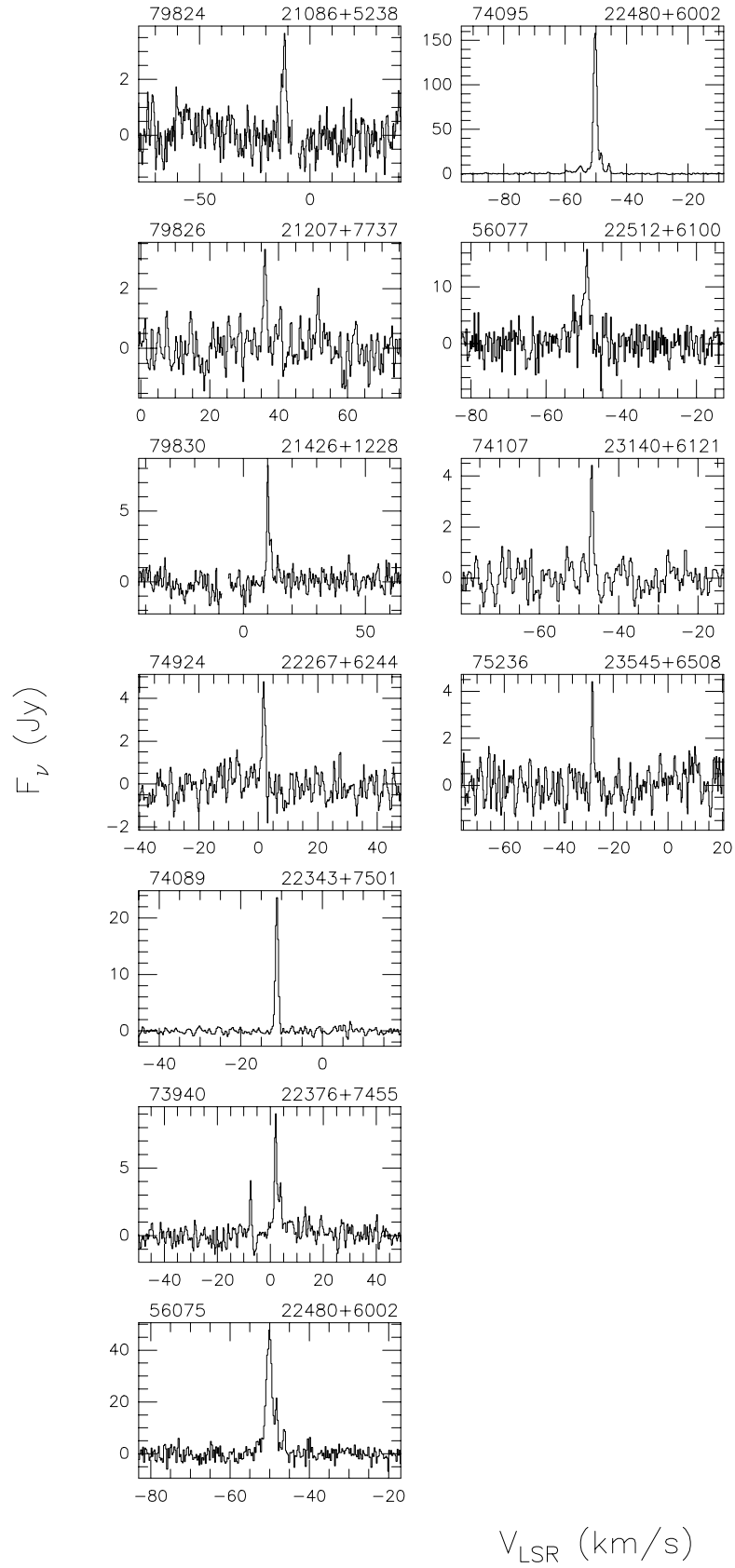


Fig. A.2. continued

References

- Benson, P. J., & Little-Marenin, I. R. 1996, *ApJS*, 106, 579
- Benson, P. J., Little-Marenin, I. R., Woods, T. C., et al. 1990, *ApJS*, 74, 911
- Brand, J., Cesaroni, R., Caselli, P., et al. 1994, *A&AS*, 103, 541
- Claussen, M. J., Wilking, B. A., Benson, P. J., et al. 1996, *ApJS*, 106, 111
- Codella, C., & Palla, F. 1995, *A&A*, 302, 528
- Codella, C., Felli, M., & Natale, V. 1996, *A&A*, 311, 971
- Codella, C., & Moscadelli, L. 2000, *A&A*, 362, 723
- Codella, C., Palumbo, G. C. C., Scappini, F., Caselli, P., & Attolini, L. 1995, *MNRAS*, 276, 57
- Colomer, F., Reid, M. J., Menten, K. M., & Bujarrabal, V. 2000, *A&A*, 355, 979
- Comoretto, G., Palagi, F., Cesaroni, R., et al. 1990, *A&AS*, 84, 179
- Dent, W. A. 1972, *ApJ*, 177, 93
- Engels, D., & Lewis, B. M. 1996, *A&AS*, 116, 117
- Han, F., Mao, R. Q., Lu, J., et al. 1998, *A&AS*, 127, 181
- Launhardt, R., Evans, N. J., II, Wang, Y., et al. 1998, *ApJS*, 119, 59
- Lewis, B. M. 1997, *AJ*, 114, 1602
- Lewis, B. M. 1999, *ApJ*, 508, 831
- Lewis, B. M., & Engels, D. 1993, *MNRAS*, 265, 161
- Lewis, B. M., & Engels, D. 1995, *MNRAS*, 274, 439
- Matthews, H. E., Olmon, F. M., Winnberg, A., & Baud, B. 1985, *A&A*, 149, 227
- Meehan, L. S. G., Wilking, B. A., Claussen, M. J., Mundy, L. G., & Wootten, A. 1998, *AJ*, 115, 1599
- Miralles, M. P., Rodriguez, L. F., & Scalise, E. 1994, *ApJS*, 92, 173
- Murtagh, F., & Heck, A. 1987, *Multivariate Data Analysis* (Dordrecht: Reidel Publ. Co.)
- Palagi, F., Cesaroni, R., Comoretto, G., Felli, M., & Natale, V. 1993, *A&AS*, 101, 153
- Palla, F., Brand, J., Cesaroni, R., Comoretto, G., & Felli, M. 1991, *A&A*, 246, 249
- Plume, R., Jaffe, D. T., Evans, N. J., II, Martin-Pintado, J., & Gomez-Gonzalez, J. 1997, *ApJ*, 476, 730
- Schreyer, K., Henning, T., Kömpe, C., & Harjunpaa, P. 1996, *A&A*, 306, 267
- Szymczak, M., & Engels, D. 1995, *A&A*, 296, 727
- Szymczak, M., & Engels, D. 1997, *A&A*, 322, 159
- Takaba, H., Ukita, N., Miyaji, T., & Miyoshi, M. 1994, *PASP*, 46, 629
- Toth, L. V., & Walmsley, C. M. 1994, *IBVS*, 4107
- Toth, L. V., & Kun, M. 1997, *IBVS*, 4492
- Wood, D. O. S., & Churchwell, E. 1989, *ApJ*, 340, 265
- Xiang, D., & Turner, B. E. 1995, *ApJS*, 99, 121
- Zinchenko, I., Pirogov, L., & Toriseva, M. 1998, *A&AS*, 133, 337